



PEOPLE'S DEMOCRATIC REPUBLIC OF ALGERIA

Ministry of Higher Education and Scientific Research

University of Amar Telidji - Laghouat



Faculty of Technology

Department of Electronics

MASTER THESIS

DOMAINE: Science & Technology

OPTION: Automation & Industrial Computing

MAILEB Moussa & MEDKOUR Mohamed Rami

Theme

Analysis and Control of DAB converter for EVs charging stations

Jury members:

HADJAISSA Aboubakeur	MCA	President
ABOUCHABANA Nabil	MCB	Examiner
BANMILOUD Mohammed	MCB	Supervisor
AMEUR Khaled	MCB	Co-Supervisor

2023 / 2024
1

Acknowledgements

We would like to express our heartfelt appreciation to our advisor, Dr. Mohammed BENMILOUD, and our co-supervisor, Dr. AMEUR Khaled , for their invaluable guidance, patience, and encouragement throughout our journey as their students. Their unwavering support and prompt responsiveness to our questions have been instrumental in our progress.

We would also like to thank the committee members: Dr. HADJAISSA Aboubakeur and Dr. ABOUCHABANA Nabil, for serving us as our committee members. We would especially like to thank everyone helps us to get this work accomplished.

We would also like to thank our families. Words cannot express how grateful we are to our parents for all of the sacrifices that they have made. Their prayers and support for us were what sustained us thus far. We would also like to thank all of our friends who supported us in preparing this project, and incited us to strive towards our goal. Finally, I would like to thank the teaching team and administrative body of the Faculty of technology for the richness and quality of their teaching, and they go to great lengths to provide their students with up-to-date training.

MAILEB Moussa & MEDKOUR Mohamed Rami

Laghouat University

September 2024

Abstract

The ongoing shift towards electric vehicles (EVs) has emphasized the need for efficient and reliable charging systems. This thesis presents an in-depth analysis of the Dual Active Bridge (DAB) converter, a key component for EV charging stations. The DAB converter's bidirectional power flow and galvanic isolation make it highly suitable for both charging and discharging scenarios, particularly in Vehicle-to-Grid (V2G) applications. The research focuses on the DAB's operational principles, power transfer mechanisms, and the implementation of control strategies to enhance efficiency and stability. Simulation results demonstrate the viability of the DAB converter in handling high power levels, ensuring fast charging, and maintaining system reliability under different operating conditions. Overall, this work contributes to the development of advanced EV charging infrastructure, aligning with the growing demand for sustainable energy solutions.

Resumé

La transition vers les véhicules électriques (VE) met en évidence la nécessité de systèmes de recharge efficaces et fiables. Cette thèse présente une analyse approfondie du convertisseur Dual Active Bridge (DAB), un composant clé des stations de recharge pour VE. Le DAB permet un flux bidirectionnel de puissance et assure l'isolation galvanique, ce qui le rend particulièrement adapté aux scénarios de charge et de décharge, notamment dans les applications Vehicle-to-Grid (V2G). La recherche se concentre sur les principes de fonctionnement du DAB, les mécanismes de transfert de puissance et la mise en œuvre de stratégies de contrôle pour améliorer l'efficacité et la stabilité. Les résultats des simulations démontrent la viabilité du convertisseur DAB pour gérer des niveaux de puissance élevés, garantir une recharge rapide et maintenir la fiabilité du système dans différentes conditions de fonctionnement. Dans l'ensemble, ce travail contribue au développement d'infrastructures de recharge avancées pour VE, en réponse à la demande croissante de solutions énergétiques durables.

ملخص

يسلط التحول إلى المركبات الكهربائية الضوء على الحاجة إلى أنظمة شحن فعالة وموثوقة. تقدم هذه الأطروحة تحليلاً متعمقاً لمحول الجسر النشط المزدوج ، وهو مكون رئيسي لمحطات شحن المركبات الكهربائية. يسمح محول الجسر النشط المزدوج بتدفق الطاقة ثنائي الاتجاه ويوفر عزلة جلفانية، مما يجعلها مناسبة بشكل خاص لسيناريوهات الشحن والتفريغ، خاصة في تطبيقات السيارة إلى الشبكة . يركز البحث على مبادئ تشغيل وآليات نقل الطاقة وتنفيذ استراتيجيات التحكم لتحسين الكفاءة والاستقرار. تُظهر نتائج عمليات المحاكاة جدوى محول الجسر النشط المزدوج للتعامل مع مستويات الطاقة العالية، وضمان الشحن السريع والحفاظ على موثوقية النظام في ظل ظروف تشغيل مختلفة. بشكل عام، يساهم هذا العمل في تطوير بنى تحتية متقدمة لشحن المركبات الكهربائية استجابة للطلب المتزايد على حلول الطاقة المستدامة.

Contents

1	Generalities of Electric Vehicle and Charging Station	7
1.1	Introduction	7
1.2	Electric Vehicle	7
1.2.1	Main elements of the EV :	8
1.3	Advantages Of The Electric Motor	9
1.3.1	Types of Electric Vehicles:	9
1.4	Charging Station	10
1.4.1	Technologies Of Charging Station:	11
1.4.2	Bi-Directional Charging	12
1.5	Bidirectional DC-DC Converters	13
1.5.1	Classification of Bidirectional DC-DC converters	15
1.6	Summary	17
2	Analysis of DAB converter	18
2.1	Introduction	18
2.2	Bidirectional DAB Converter	18
2.2.1	Description of DAB Converter	18
2.2.2	Power transfer principle	19
2.3	Phase-Shift Modulation for DAB	20
2.3.1	Single phase shift (SPS)	21
2.3.2	Dual-Active Bridge - Switching Sequence	21
2.3.3	Dual-Active Bridge - Zero Voltage Switching (ZVS)	26
2.3.4	Power Flow Control (general case)	28
2.3.5	Output power calculation (In one direction)	30

2.3.6	DAB component selection	33
2.4	Open Loop simulation	37
2.4.1	System and simulation configuration	37
2.4.2	Simulation results	38
2.5	Summary	40
3	DAB Charger Control	41
3.1	Introduction	41
3.2	Problem statement	41
3.3	Closed loop control	43
3.3.1	Design of PI control	43
3.3.2	System and simulation configuration	44
3.3.3	Simulation results	45
3.4	Summary	49

List of Figures

1.1	Main elements of the EV	8
1.2	Electric Motor	9
1.3	Charging Station	11
1.4	Bi-Directional Charging	13
1.5	Classification of bidirectional DC–DC converters.	15
1.6	Typical Non-isolated circuit diagram.	15
1.7	Structure of Isolated Bidirectional DC-DC Converter (IBDC)	17
2.1	Dual Active Bridge	19
2.2	Power transfer between two AC voltage sources	19
2.3	Power transfer between two AC voltage sources via a transformer	20
2.4	Interval 1: Negative Inductor Current	22
2.5	Interval 1: Positive Inductor Current	22
2.6	Interval 2	23
2.7	Interval 3: Positive Inductor Current	24
2.8	Interval 3: Negative Inductor Current	24
2.9	Interval 4	25
2.10	Gate Signals, Transformer Primary and Secondary Voltages, and Inductor Current	25
2.11	ZVS Transition in Secondary Side - Capacitor	26
2.12	ZVS Transition in Secondary Side - Diode ZVS Transition in Secondary Side - Diode	27
2.13	ZVS Transition in Primary Side - Capacitor	28

2.14 ZVS Transition in Primary Side - Diode	
- Diode	28
2.15 Power transfer in DAB converter in function of the phase shift	29
2.16 Dual Active Bridge (R_L load)	30
2.17 Wave curves of input voltage (V_1), output voltage (V_2), inductor voltage(V_L) and Current (i_L)	30
2.18 Output Current waveform	31
2.19 Dual Active Bridge R_L load	33
2.20 Three cases of i_L (inductance current)	33
2.21 Wave curves of inductor current (i_L), Output current(i_o) and output average current (I_o)	35
2.22 Simulation Open Loop of DAB converter	38
2.23 Phase shift angle	38
2.24 Current of the inductance(i_L), input voltage (V_1) and output voltage (V_2)	39
2.25 Output Power	39
3.1 Dual Active Bridge	42
3.2 Block diagram of our closed loop system	44
3.3 Simulation Closed Loop of DAB converter	45
3.4 Power request	46
3.5 Phase shift angle	46
3.6 IGBTs' waveforms with SPS in G2V mode for $V_b=250V$ and $P=7,5kW$	47
3.7 current of the inductance(i_L), output voltage of the first bridge(V_1), the input voltage of the second bridge(V_2)	47
3.8 Comparison between power request and transfer power	48
3.9 Comparison between power request and actual transferred power	48

General Introduction

Importance of Electric and Hybrid Electric Vehicles

The transition from traditional vehicles powered by internal combustion engines to electric vehicles (EVs) and hybrid electric vehicles (HEVs) has become a pivotal solution in addressing the urgent environmental and energy challenges facing our planet. The transportation sector significantly contributes to global greenhouse gas emissions, with vehicles powered by fossil fuels being a primary source of air pollutants and carbon dioxide emissions. As awareness of climate change and its consequences grows, the urgency to mitigate these impacts has led governments, organizations, and individuals to seek cleaner alternatives. Electric and hybrid vehicles present a viable solution, not only because they produce zero tailpipe emissions but also due to their potential for significant reductions in overall emissions when charged using renewable energy sources. This transition is not merely a trend but a necessary shift towards achieving global sustainability goals.

In response to this growing recognition of the environmental benefits of electric mobility, governments worldwide are actively promoting the adoption of electric and hybrid vehicles through various incentives. These include tax credits, rebates, and substantial investments in charging infrastructure. Such policies aim to foster a sustainable transportation ecosystem that can help mitigate climate change while also promoting energy security and reducing dependency on fossil fuels. Additionally, public awareness campaigns and educational initiatives are helping to inform consumers about the benefits of electric vehicles, contributing to a positive perception of these technologies. As the market for EVs continues to expand, the automotive industry is undergoing a transformative change, with major manufacturers committing to electrifying their

fleets and investing in new technologies to meet growing consumer demand.

Autonomy and Recent Developments

A critical factor influencing consumer acceptance of electric vehicles is their autonomy, defined as the maximum distance an EV can travel on a single charge. Historically, range anxiety—the fear of running out of charge without access to a charging station—has been a significant barrier to adoption. However, significant advancements in battery technology and vehicle design have led to notable improvements in autonomy. Modern electric vehicles are now capable of achieving impressive ranges, often exceeding 300 miles on a single charge. This enhanced range aligns closely with the average daily driving distance for most consumers, making electric vehicles a more practical choice for everyday use.

Recent developments in battery technology have played a pivotal role in enhancing the autonomy of electric vehicles. The introduction of lithium-ion batteries has revolutionized energy storage solutions, providing higher energy density and efficiency compared to traditional lead-acid batteries. These advancements allow manufacturers to produce vehicles that can travel longer distances between charges while maintaining performance. Furthermore, ongoing research into solid-state batteries holds the promise of even greater improvements in energy density, charging speed, and safety. Solid-state batteries utilize a solid electrolyte instead of a liquid one, potentially offering higher energy storage capacities and reduced risks of fire or leakage. As a result, the latest electric vehicles are becoming increasingly competitive with traditional gasoline-powered cars, addressing the concerns of range anxiety and promoting wider adoption.

Challenges of Charging Time

Despite these advancements in autonomy, the challenge of charging time remains a significant obstacle to the widespread acceptance of electric vehicles. While traditional gasoline-powered vehicles can be refueled in a matter of minutes, the time required to recharge an electric vehicle can range from several hours to a whole day, depending on the charger and battery capacity. This discrepancy in refueling time can deter

consumers, particularly those who rely on their vehicles for daily transportation and seek the convenience that comes with quick refueling options.

To address this challenge, the development of fast-charging technology has gained momentum in recent years. DC fast chargers, for example, utilize high-power direct current (DC) to rapidly recharge EV batteries, significantly reducing charging times. By bypassing the vehicle's onboard AC-to-DC converter, these chargers can supply high power directly to the battery, allowing for an 80% charge in as little as 30 minutes. This rapid charging capability is crucial for long-distance travel and the expansion of charging infrastructure, particularly along highways and in urban areas where drivers may need to quickly recharge their vehicles. The implementation of fast-charging networks is becoming increasingly vital as more consumers transition to electric vehicles, ensuring that charging stations are readily available and accessible.

Types of EV Chargers and Static Converters

Electric vehicle chargers can be categorized based on the type of static converters employed in their design. The primary types include AC chargers and DC fast chargers. AC chargers, which include Level 1 and Level 2 chargers, are the most common type of chargers available. Level 1 chargers typically use standard 120V outlets, providing a slow charge suitable for home use and taking several hours to fully recharge a vehicle. Level 2 chargers operate at 240V and are commonly found in public charging stations, offering faster charging capabilities. While AC charging is convenient for overnight charging at home, it generally requires longer times compared to DC fast charging, which is essential for those who need to recharge quickly during a long journey.

DC fast chargers are designed to deliver high-power direct current directly to the vehicle's battery, significantly reducing charging times. By bypassing the vehicle's onboard AC-to-DC converter, DC fast chargers can supply power directly to the battery, making them ideal for commercial applications and long-distance travel. These chargers utilize advanced power electronics and sophisticated control systems to manage the high-power levels required for fast charging. With the increasing demand for electric vehicles, the deployment of DC fast chargers is becoming essential to provide the necessary infrastructure for a growing user base.

Vehicle-to-Grid (V2G) Technology

With the advent of Vehicle-to-Grid (V2G) technology, bidirectional chargers have gained prominence as a critical component of modern electric vehicle infrastructure. These chargers enable energy flow in both directions, allowing electric vehicles to draw power from the grid and return energy when necessary. This bidirectional capability not only enhances grid stability but also allows electric vehicles to serve as mobile energy storage units, supporting renewable energy integration and demand response strategies. V2G technology is reshaping the interaction between electric vehicles and the power grid, providing a dynamic solution for energy management.

The integration of V2G technology allows electric vehicles to play an active role in the energy ecosystem, contributing to the stabilization of the grid during peak demand periods. When electricity demand surges, electric vehicles can discharge energy back into the grid, helping to balance supply and demand. This capability is particularly beneficial in regions with high penetration of renewable energy sources, such as solar and wind, where energy generation can be intermittent. By enabling electric vehicles to return energy to the grid, V2G technology supports a more sustainable and resilient energy infrastructure.

To facilitate V2G applications, the use of bidirectional DC-DC converters is essential. These converters enable efficient energy transfer in both directions while ensuring galvanic isolation for safety and reliability. Galvanic isolation is vital in preventing ground loops and minimizing electrical noise, which enhances overall system stability. As V2G technology continues to evolve, the need for advanced power electronics solutions, including bidirectional converters, will become increasingly critical in supporting the integration of electric vehicles into the smart grid.

The Dual Active Bridge (DAB) Structure

Among the various converter topologies employed in electric vehicle chargers, the Dual Active Bridge (DAB) has garnered significant attention for its suitability in both charging applications and V2G integration. The DAB topology consists of two active power converter stages, one on the input side and one on the output side, connected by

a high-frequency transformer. This configuration facilitates bidirectional power flow while providing galvanic isolation, making it ideal for electric vehicle charging applications that require both efficiency and safety.

The DAB topology offers numerous advantages, including high efficiency, compact design, and soft-switching capabilities that minimize switching losses and thermal stress on components. The use of a high-frequency transformer in the DAB also allows for reduced size and weight compared to traditional transformer designs, making it an attractive option for electric vehicle applications where space and weight are critical considerations. Additionally, the modular nature of the DAB allows for easy scalability, enabling it to adapt to varying power requirements, which is particularly advantageous in the context of fast-charging solutions and V2G applications.

As the demand for advanced charging solutions continues to grow, the DAB topology is poised to play a crucial role in the future of electric mobility. Its ability to handle high power levels while maintaining efficiency makes it a compelling choice for electric vehicle chargers, particularly in applications that require rapid charging and bidirectional energy transfer. The integration of DAB technology into electric vehicle charging systems not only enhances performance but also supports the broader goals of sustainability and energy efficiency.

Objective of the Thesis

This master thesis focuses on the analysis and control of the Dual Active Bridge (DAB) in the context of electric vehicle chargers. The primary objective is to explore the operational principles of the DAB topology, analyze its performance characteristics, and develop effective control strategies to optimize its functionality for electric vehicle applications. By delving into the intricacies of the DAB, this work aims to contribute valuable insights to the ongoing evolution of electric vehicle charging technologies.

Thesis Outline

The structure of this thesis is organized into three chapters, each addressing specific aspects of the analysis and control of the Dual Active Bridge in electric vehicle chargers.

The first chapter provides a comprehensive overview of electric vehicles and the associated charging infrastructure. It delves into the fundamental concepts of EV technology, including their operation, benefits, and the various types of charging stations. This chapter establishes the context for understanding the importance of efficient charging systems and sets the stage for the subsequent analysis of power conversion technologies.

The second chapter focuses on the analysis of DAB converters, particularly within an open-loop system configuration. It examines the operational principles of DAB converters, including their efficiency, performance characteristics, and the challenges associated with their implementation in EV charging stations. This chapter aims to provide a detailed technical understanding of how DAB converters function and their potential advantages and limitations in an open-loop setup.

Building on the analysis from the previous chapter, the third chapter addresses the control of DAB converters using a Proportional-Integral (PI) controller. This chapter explores how PI control can be employed to regulate the DAB converter's performance by managing the difference between the power request and the power changes. The focus here is on improving system stability and response, ensuring that the charging station operates efficiently and meets the dynamic demands of EV charging.

Chapter 1

Generalities of Electric Vehicle and Charging Station

1.1 Introduction

In this chapter, we will delve into the fundamental aspects of electric vehicles. We will explore the advantages of electric motors, which include significant environmental benefits, improved efficiency, and lower operating costs. Additionally, we will examine the critical infrastructure that supports the widespread adoption of EVs, focusing on the development and expansion of charging stations

1.2 Electric Vehicle

An electric vehicle (EV) is an automobile that is powered by one or more electric motors, using energy stored in rechargeable batteries or another energy storage device. EVs are distinct from conventional internal combustion engine vehicles, as they do not rely on the combustion of fossil fuels to generate power. Instead, they utilize electricity as their primary source of energy, which can be obtained from various sources, including the electrical grid, renewable energy sources such as solar or wind power, or onboard generators such as fuel cells. Electric vehicles offer the potential for reduced greenhouse gas emissions and air pollution compared to traditional vehicles, contributing to efforts to mitigate climate change and improve air quality.[1] EVs play a more and more

important role in road transportation. According to the types of energy sources (gasoline or diesel, battery, and hydrogen fuel) and the propulsion devices (engine and motor). It can be seen that EVs can be generally classified as the hybrid EV (HEV), the battery EV (BEV), and the fuel-cell EV (FEV). Meanwhile, the HEV can be further classified as the conventional HEV (including the micro, mild, and full hybrids), the plug-in HEV (PHEV), and the range-extended EV (REV). All kinds of EVs enjoy the definite merit of energy diversification. It can be found that the PHEV, the REV, and the BEV can be directly fed by electricity from the power grid. These EVs are called GEVs which can be directly plugged into the power grid to absorb energy as loads or to deliver energy as resources.[2]

1.2.1 Main elements of the EV :

The constitution of the EV and the basic components are shown in figure:

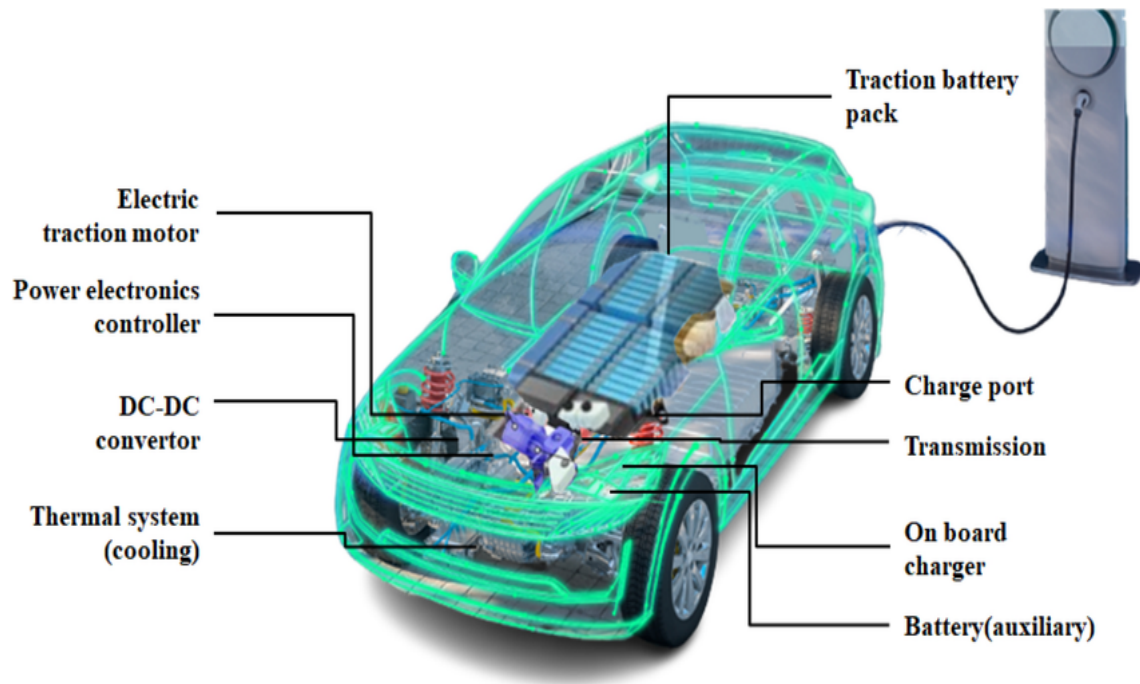


Figure 1.1: Main elements of the EV

1.3 Advantages Of The Electric Motor

the advantages of the electric motor are numerous. It only has one moving part known as the rotor. Therefore, it can be relatively light, compact and inexpensive. The electric motor can last a long time without requiring maintenance. The energy efficiency of the motor can be close to 100% and you can win back energy when braking. Because of this, the average electric car is four times more efficient than the average conventional car. And if you compare sports cars the electric car is up to twenty times more efficient. So oversizing an electric engine does not materially reduce efficiency and the engines are cheap and light. That is one reason why, in practice, electric vehicles can accelerate much faster. For health and climate, the biggest advantage is clear: it can run on renewable energy and the motor itself has zero emissions. [3].

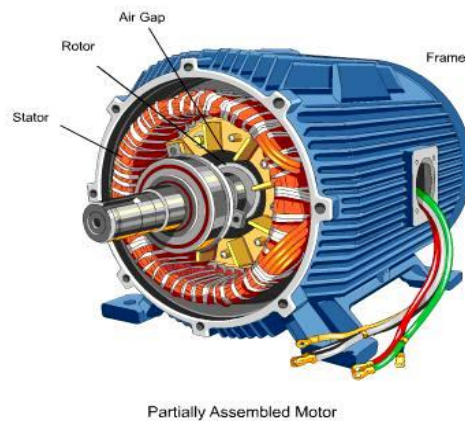


Figure 1.2: Electric Motor

1.3.1 Types of Electric Vehicles:

Electric vehicles (EVs) come in various forms, catering to different needs and preferences. Here are the main types:

- **Battery Electric Vehicles (BEVs):** Electric cars based solely on batteries are called BEV power. Not powered by internal combustion motor, battery capacity directly affects the BEV range. Usually, BEV can cover 100-250km in one charge, BEV advantages include simple construction, easy operation and completely noise-free. It is also environmentally friendly due to the absence of any green-

house gas emissions. The only drawback is the shorter range of each shipment making it along with its advantages an ideal option for the urban family.[4]

- **Plug-in Hybrid Electric Vehicles (PHEVs):** Plug-in hybrids were developed to increase the range of HEVs (Gao and Ehsani 2010). PHEVs utilize an electric motor and a battery that could be charged via the power grid. The battery is also supported by an ICE that can recharge or replace when the vehicle is running on a low battery. Fuel saving is higher in comparison to HEVs as PHEVs utilize electricity directly from the power grid.[4]
- **Hybrid Electric Vehicles (HEVs):** The International Technical Committee 69 (Electric Road Vehicles) defined HEV as “Vehicles utilizing two or more energy sources or storage such that at least one provides electrical energy” (Chan 2002). HEV commonly has an engine with a fuel tank and an electric motor with a battery. Energy is solely derived from gasoline and from regenerative braking. HEVs could be further be classified into four types: - Series hybrids, - Parallel hybrids, - Series-parallel hybrids, and - Complex hybrids. The range of HEV is higher than BEV but it has few disadvantages of being expensive to operate the BEV and also cannot be conveniently charged at home.[4]
- **Fuel Cell Electric Vehicles (FCEVs):** A fuel cell has properties of both a battery and an ICE; it generates electricity from an electrochemical reaction like a battery and it can run indefinitely if it is supplied with a source fuel (hydrogen) similar to an ICE (Matthey 2013). The automotive industry uses proton exchange membrane fuel cell (PEMFC) as its fuel type. FCEVs have a longer range compared to most battery electric vehicles and can be refueled relatively quickly, They emit only water vapor and are considered zero-emission vehicles.[4]

[5]

1.4 Charging Station

A charging station is a device that provides electrical power to recharge plug-in electric vehicles, where the charging equipment for EVs plays a critical role in their develop-

ment, grid integration and daily use: a charging station generally includes charge cord, charge stand, attachment plug, power outlet and vehicle connector and protection system. The configuration of the charging station can vary from Country to Country depending on frequency, voltage, electrical grid connection and standards.[6].

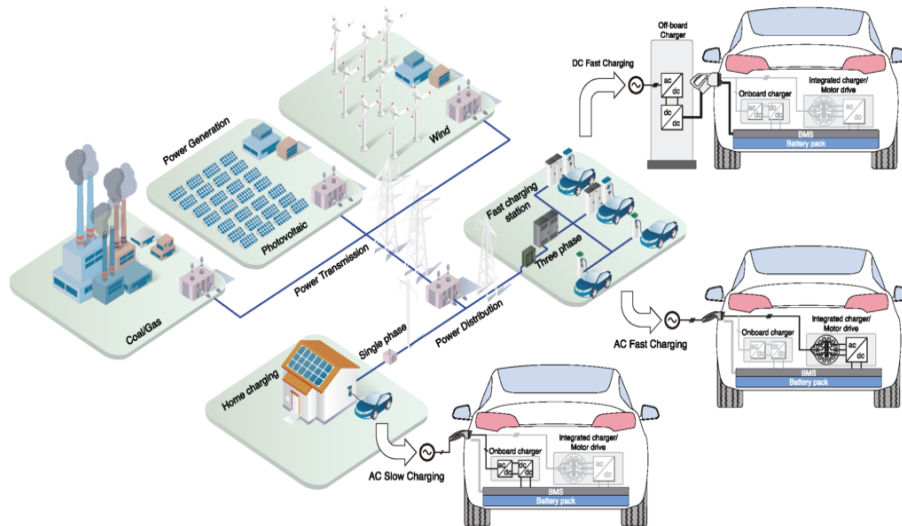


Figure 1.3: Charging Station

1.4.1 Technologies Of Charging Station:

Electric vehicle charging stations utilize various technologies to efficiently and safely charge electric vehicles. Here are some of the key technologies employed in charging stations:

- **AC Charging:** Alternating current (AC) charging is the most common method used for charging electric vehicles. AC charging stations deliver power to the vehicle's onboard charger, which converts AC power to DC power to charge the vehicle's battery. AC charging is typically available in two levels:

Level 1 Charging: Uses a standard 120-volt AC household outlet. It provides a slow charging rate, suitable for overnight charging.[7]

Level 2 Charging: Utilizes a 240-volt AC supply, offering faster charging compared to Level 1. Level 2 charging stations are commonly installed in residential, commercial, and public locations.[7];

- DC Fast Charging (DCFC): DC fast charging station provides direct current (DC) for car battery, overtaking charger. DC Fast chargers are integrated into commercial and public places. This type of charging provides 80% charging in 10-15 minutes. It's one of the most promising technologies that will create a huge impact in electric vehicle charging stations. There are many types of fast charging that we mention CHAdeMO, CCS (charging system), Tesla Supercharger.[7]
- Wireless Charging: Utilizes inductive charging technology, allowing EVs to be charged without physical connectors. This method is gaining popularity for its convenience and is being explored for dynamic charging, where EVs can be charged while driving on equipped roads[7]

1.4.2 Bi-Directional Charging

- Grid-to-Vehicle (G2V) refers to the process of transferring electrical energy from the grid to electric vehicles (EVs) for the purpose of charging their batteries. This term is often used in the context of smart grid technologies and electric vehicle charging infrastructure.
- (Vehicle-to-Grid, V2G): Bi-directional charging enables electric vehicles to not only receive power from the grid but also to discharge stored energy back to the grid when needed. This technology allows electric vehicles to function as mobile energy storage units, contributing to grid stability and supporting renewable energy integration. V2G systems require compatible charging infrastructure and vehicle-to-grid communication protocols.[8]

G2V & V2G systems typically involve communication between the grid, charging infrastructure, and EVs to manage the charging process efficiently. This communication allows for features such as demand response, where EV charging can be coordinated to minimize strain on the grid during peak demand periods, and time-of-use pricing, where charging rates vary based on electricity demand and pricing.

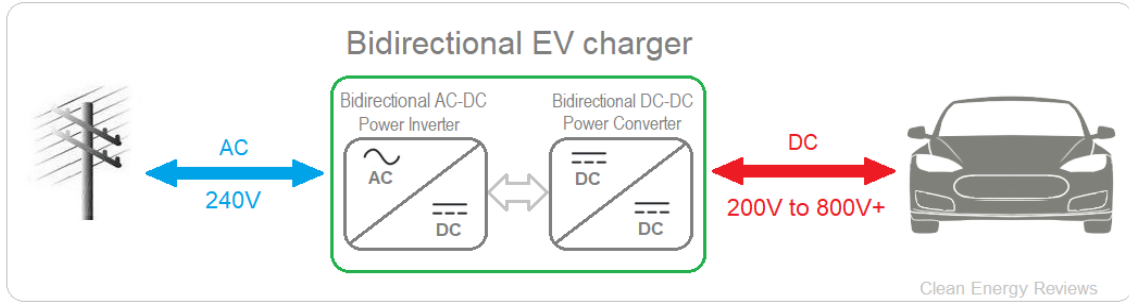


Figure 1.4: Bi-Directional Charging

1.5 Bidirectional DC-DC Converters

The continuous flow of power is an important concern when it comes to renewable energy systems; therefore, bidirectional DC–DC converters are employed to interface storage systems with the energy resource and load by reducing or eliminating the fluctuation in the output of renewable energy systems as a result of variations in climate conditions. They are also used between the energy source and motor supplied by batteries [9]. In medium-power rank devices where familiar and efficient energy storages are supercapacitors and batteries, the energy exchange between the storage device and the other components of the system requires the presence of a DC–DC converter, and such converters must have a bidirectional power flow capability and should have an adaptable control in all operation modes [10]-[11]. Only one-directional power flow management can be achieved with a conventional buck–boost converter when compared with bidirectional power, which can flow in two directions (forward (FW) and backward (BW)). Bidirectional DC converters (BDCs) are a device for either stepping up or stepping down voltage level; it can facilitate two-directional power flow (both forward and backward power flows). Bidirectional DC–DC converters are mainly used to manage the flow (forward and backward) of power in DC bus voltage where power flow is in both directions. The conversion of the conventional DC–DC converter into a bidirectional converter can be achieved using a bidirectional switch with a diode, with the current flow in both paths being accepted by anti-parallel with an insulated-gate bipolar transistor (IGBT) or metal–oxide–semiconductor field-effect transistor (MOS-FET) employing a controlled switching procedure. Bidirectional DC/DC converters

are of two kinds based on existing galvanic isolation between the input and the yield; they are isolated bidirectional DC (IBDC) and non-isolated bidirectional DC (NIBDC) [12]-[13]. The adaptability of the energy storage system can be improved by using a high-frequency isolated DC-DC converter to replace the line-frequency transformer. The circuits of most DC-DC converters are arranged asymmetrically to couple the two DC connections to various voltages, from tens of volts to hundreds of volts [14]. Bidirectional converters have become more popular, as opposed to traditional unidirectional converters, as they permit power flow in both directions.

They are mostly used in hybrid electric vehicles (HEVs), electric vehicles (EVs), uninterruptible power supplies (UPS), smart grids, renewable energy systems (RESs), and aerospace applications; they are also used in other systems that require batteries [15].

Utilized DC-DC converter in EVs should be capable to operate in bidirectional mode. This property enables the converter to transmit power from battery-side to motor-side and vice versa. The use of a Bi-directional dc-dc converter fed dc motor drive devoted to electric vehicles (EVs) application allows a suitable control of both motoring and regenerative braking operations, and it can contribute to a significant increase the drive system overall efficiency. Recently many Bidirectional dc-dc converter topologies have been reported with soft switching technique to increase the transfer efficiency. Bi-directional converters using coupled inductor were introduced for soft-switching technique with hysteresis current controller. For minimizing switching losses and to improve reliability, zero voltage-switched (ZVS) technique and zero-current-switched (ZCS) technique were introduced for Bi-directional converter. A multiphase Bi-directional converter is suitable for high power application. To achieve high voltage rating or current rating more number of converters can be connected in series or parallel with low switching frequency. A unified current controller was introduced for Bi-directional dc-dc converter which employs complementary switching between upper and lower switches.[16]

1.5.1 Classification of Bidirectional DC-DC converters

As mentioned in the preceding section, bidirectional DC-DC converters are of two types—IBDC and NIBDC—as they been classified in Figure 1.5

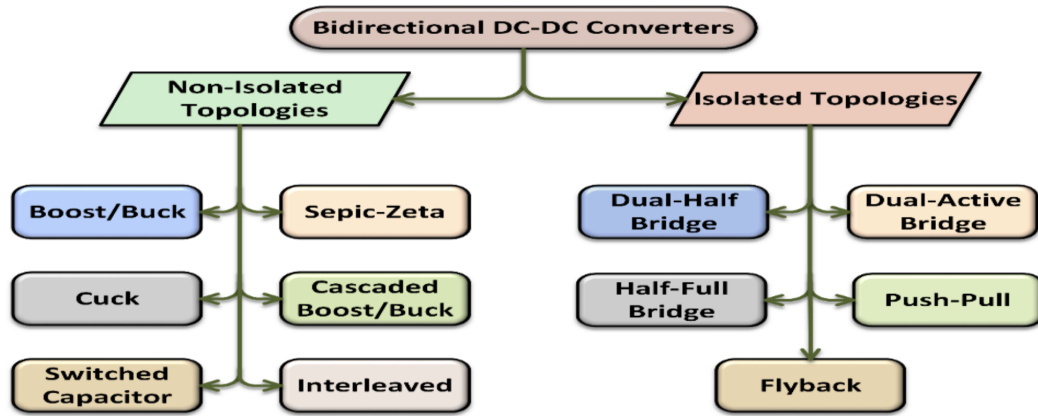


Figure 1.5: Classification of bidirectional DC-DC converters.

The non-isolated topologies transfer the power without magnetic isolation. Though the non-isolated topologies do not use a transformer and lack the advantages of galvanic isolation such as high step-up voltage gain ratio, they benefit from a simpler configuration and do not suffer from disadvantages of galvanic isolation such as magnetic interference or high weight. These characteristics make them suitable when size and weight are important concerns in particular applications.[17]

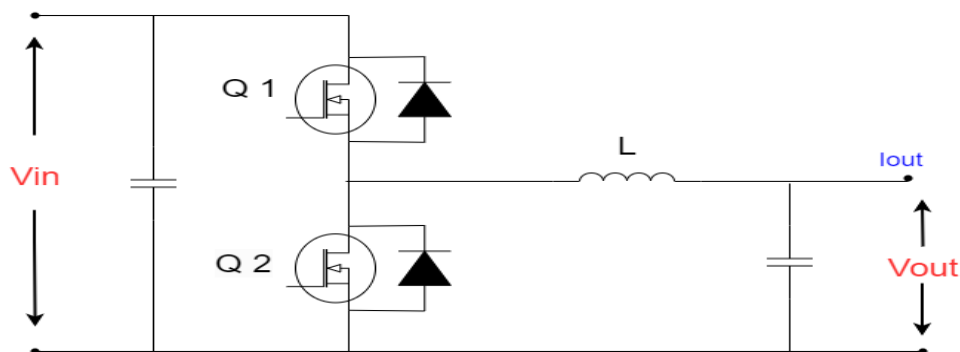


Figure 1.6: Typical Non-isolated circuit diagram.

There are no secure galvanic isolation standards in the non-isolation BD converter; hence, most applications use IBDCs rather than NIBDCs. IBDCs rely on a great

frequency transformer to offer galvanic isolation. In numerous applications and with regard to overburden for the safety of the source, galvanic isolation is vital, in addition, to reduce commotion and voltage coordination between conditions [18]. Most IBDCs have similar structures, as shown in Figure 10. This converter works in two stages: great frequency switching by the DC–AC converter and the utilization of a high-frequency transformer to maintain the galvanic isolation between two sources, as well as the utilization of transformers to coordinate the voltage between various stages for the best possible plan and enhancement of various stages [10, 19]. Isolated bidirectional DC–DC converters with a basic structure were proposed by [10] to function as a flexible interface for power processing between the energy storage system and the other system components. The IBDC has some benefits, such as having no need for active or passive elements in soft switching. Secondly, the structure of the transformer is simple; therefore, maintenance and designing tasks are also simple. Additionally, both parts face the same issue of stresses in the switch currents. This approach also relies on the average current control method or peak current mode control. The absence of extra inactive components ensures quicker dynamic conduct. On the other hand, this converter has drawbacks, such as losing soft switching in light load conditions, and this control is sensitive to a slight variety of flux, particularly when bus voltages are high. An additional weakness is that currents flowing in DC buses hold great ripple content; this demands fitting filtering circuits, which makes the circuit complex [19, 20]. An isolated converter has many topologies, such as the push–pull IBDC, forward IBDC, fly-back IBDC, dual half-bridge IBDC, Cuk IBDC, and dual active full-bridge IBDC [21]-[22]. The efficiencies of the full-bridge and half-bridge topologies endear them to many applications [23], [24]

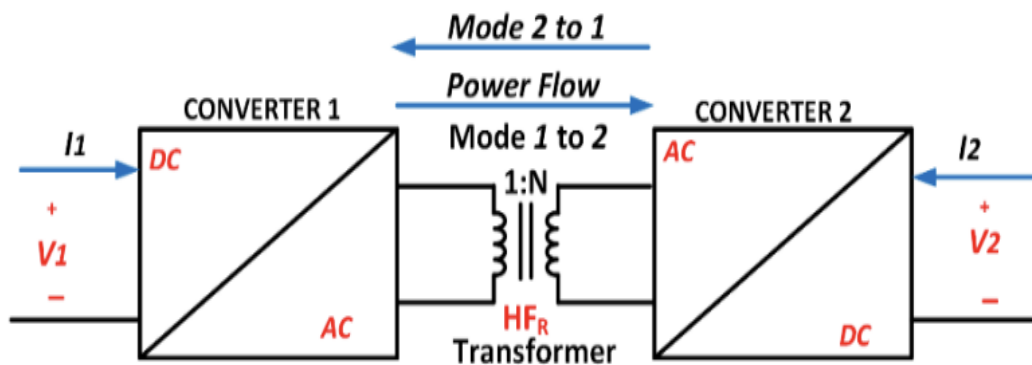


Figure 1.7: Structure of Isolated Bidirectional DC-DC Converter (IBDC)

1.6 Summary

This chapter introduces the fundamental concepts of electric vehicles, highlighting their advantages over traditional internal combustion engine vehicles. Electric motors, the primary drivers in EVs, offer benefits such as high efficiency, reduced emissions, and lower maintenance costs. The chapter categorizes various types of EVs, including Battery Electric Vehicles (BEVs), Plug-in Hybrid Electric Vehicles (PHEVs), and Hybrid Electric Vehicles (HEVs), and discusses their specific advantages and limitations.

Additionally, the chapter covers the development of charging infrastructure, which is critical for supporting the widespread adoption of EVs. Different types of charging stations are explored, ranging from slow AC chargers to fast DC chargers. The introduction of bidirectional charging systems is emphasized, particularly in the context of Vehicle-to-Grid (V2G) technology, which allows energy to flow between the grid and the vehicle. The chapter concludes by introducing the role of bidirectional DC-DC converters in facilitating power transfer and managing energy storage systems in EVs.

Chapter 2

Analysis of DAB converter

2.1 Introduction

In the realm of power electronics, DC/DC converters play a crucial role in energy management and conversion. They are essential for efficiently transforming electrical energy between different voltage levels while maintaining high performance and reliability. This chapter delves into various types of DC/DC converters, with a particular focus on bidirectional converters and their simulations. We will explore the Bidirectional DC/DC Converters, the Bidirectional Dual Active Bridge (DAB) Converter, emphasizing their operational principles, simulation models, and practical applications.

2.2 Bidirectional DAB Converter

2.2.1 Description of DAB Converter

A "dual active bridge" (DAB) is a type of bi directional dc dc converter used in power electronics. It consists of two active bridges connected by an isolation transformer. Each active bridge contains high-frequency switches, usually MOSFETs or IGBTs, allowing bidirectional power flow. DAB topology features desirable performance characteristics including galvanic isolation, high power density, low device stresses, and bidirectional operation. [25]

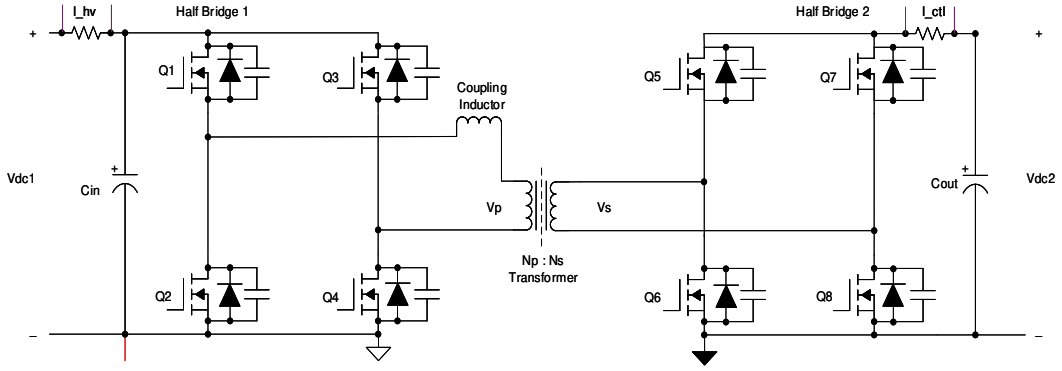


Figure 2.1: Dual Active Bridge

2.2.2 Power transfer principle

When two AC sources are connected to each other via an inductor, as in figure 2.2, the power flow direction between them depends on the phase shift between the two sources.

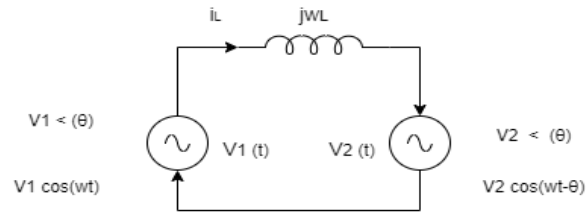


Figure 2.2: Power transfer between two AC voltage sources

$$v_L(t) = L \frac{di_L(t)}{dt} = v_1(t) - v_2(t) \quad (2.1)$$

$$i_L(t) = \frac{1}{L} \left[\int v_1(t) dt - \int v_2(t) dt \right] \quad (2.2)$$

$$v_1(t) = V_1 \sin(\omega t) \quad \text{and} \quad v_2(t) = V_2 \sin(\omega t - \theta) \quad (2.3)$$

$$P_2(t) = v_2(t)i_L(t) \quad (2.4)$$

$$P = \langle P_2(t) \rangle = \frac{1}{T} \int_0^T P_2(t) dt = \frac{V_1 V_2}{\omega L} \sin(\theta) \quad (2.5)$$

When $(0 \leq \theta \leq \pi)$ the power flows from $V_2 \rightarrow V_1$,

When $(\pi < \theta < 2\pi)$ the power flows in the other direction from $V_1 \rightarrow V_2$.

The same idea can be extended and applied in the following circuit. As both input and output sources are alternatives, a transformer can be inserted as illustrated in figure 2.3

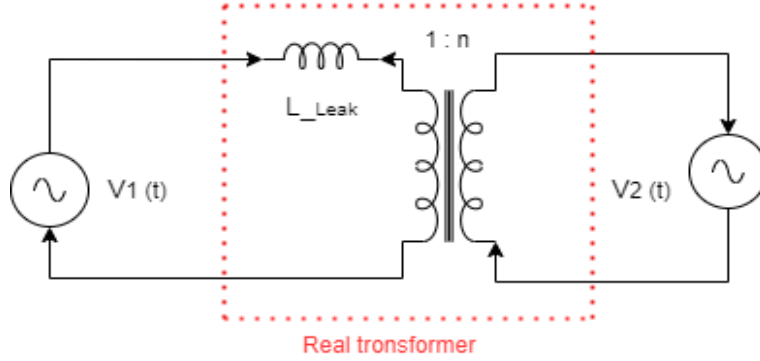


Figure 2.3: Power transfer between two AC voltage sources via a transformer

The inductor in this circuit represents the leakage inductor of the transformer. If the leakage inductor is too small another one is added in series with the transformer. The power transfer principle can be applied to the Dual Active bridge as well.

2.3 Phase-Shift Modulation for DAB

The modulation schemes that are commonly employed to regulate the output voltage and transferred power of DAB converter include: single phase shift (SPS) modulation, extended phase shift (EPS) modulation, Dual phase shift (DPS) modulation, and triple phase shift (TPS) modulation. This paper focuses on the DAB converter under SPS control, which is most widely used. The SPS modulation scheme has only one control variable—the phase shift ratio between the H1 and H2.

2.3.1 Single phase shift (SPS)

SPS is a very popular control scheme of DAB. Voltage and power flow direction on both sides of the highfrequency transformer is maintained through the SPS phase shift. SPS control provides many advantages like less, high dynamic, soft-switching control and ease to access etc.when the voltage amplitude of both the side of SST is unbalanced due to large circulating current then there is the increment in resultant RMS and maximum current that increase the power losses and reduce its efficiency. These problems are removed by using the SPS control technique.[26]In SPS modulation, the control of power transfer is achieved by shifting the phase of the gate drive signals between the primary and secondary side full-bridge converters. This phase shift creates a time difference between the voltage waveforms on the primary and secondary sides, which in turn controls the direction and amount of power flow.

2.3.2 Dual-Active Bridge - Switching Sequence

In a single-phase, dual-active bridge, primary and secondary bridges are controlled simultaneously. All switches operate at 50% duty ratio. The diagonal switches turn on and turn off together so that the output of each bridge is a square wave. The switching sequence of the converter is elaborated in detail in this section. The switching sequence is divided into four intervals based on the inductor current waveform and phase shift between the voltages at the primary and secondary of the transformer. The voltage and the current waveforms are depicted in Figure 2-14. During interval one, the inductor current waveform is both positive and negative, and hence, the current commutation follows the scheme shown in Figure 2-8 and Figure 2-9. During this interval, switches Q1 and Q4 in the primary and switches Q6 and Q7 in the secondary conduct current.[27]

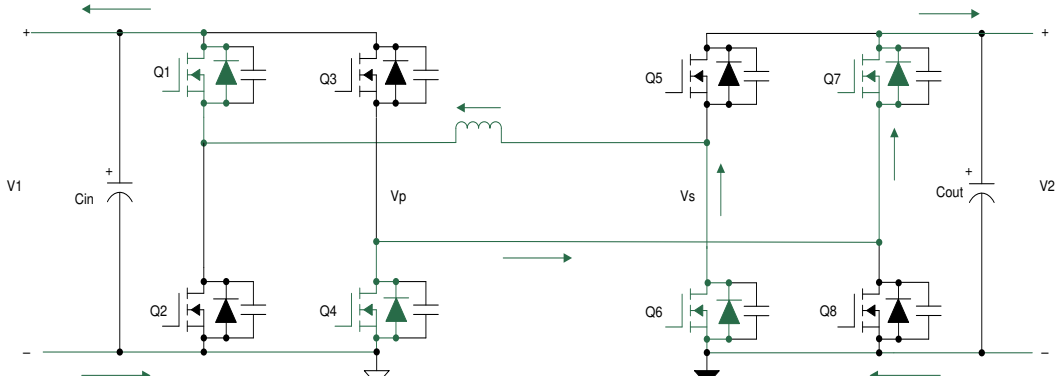


Figure 2.4: Interval 1: Negative Inductor Current

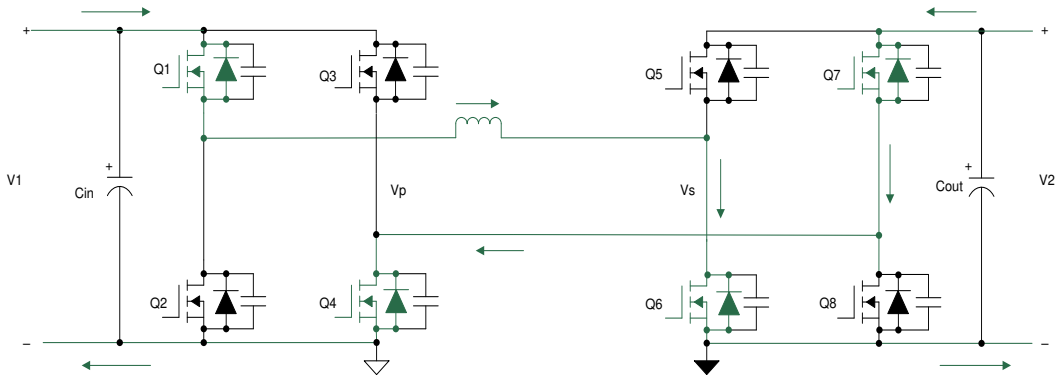


Figure 2.5: Interval 1: Positive Inductor Current

During this interval, the voltage across the primary, V_p , is equal to V_1 , and the voltage across the secondary, V_s , is equal to V_2 . The difference between these voltages appears across the leakage inductor, and the slope of the current during this interval can be approximated by Equation 2.25.[27]

$$\frac{di(t)}{dt} = \frac{V_1 + V_2}{L} \quad (2.6)$$

During interval two, the inductor current is positive. The voltage across the transformer primary is positive and is equal to V_1 , and the voltage across the secondary winding is positive and is equal to V_2 . Hence, the difference of these two voltages appears across the leakage inductor, and the slope of the rising current during this interval can be calculated by Equation 2.26.[27]

$$\frac{di(t)}{dt} = \frac{V_1 - V_2}{L} \quad (2.7)$$

During this interval, switches Q1 and Q4 remain turned on, but as the voltage across the secondary is now V_2 with the inductor current positive, switches Q5 and Q8 turn on to conduct current. There is a small dead time period between the turn off of Q6 and Q7 and the turn on of Q5 and Q8. During this dead time, the phenomenon of zero voltage switching (ZVS) occurs, which is explained in detail in the following section. The commutation sequence for the second interval is shown in Figure 2-10.[27]

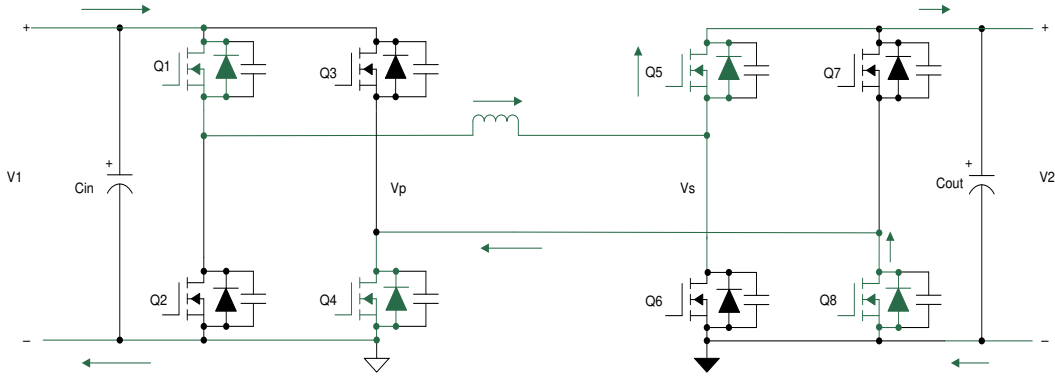


Figure 2.6: Interval 2

During interval three, the inductor current starts ramping down from its positive peak to a negative value as shown in Figure 2-10. In this interval, the voltage across the primary is $-V_1$, and the voltage across the secondary is V_2 . The difference of these voltages, which is $(-V_1 - V_2)$, appears across the inductor. Hence, the current ramps down with a negative slope as shown in Equation 2.27.

$$\frac{di(t)}{dt} = -\frac{V_1 + V_2}{L} \quad (2.8)$$

During this interval, switches Q5 and Q8 continue to remain turned on, but as the voltage across the primary is now $-V_1$, switches Q2 and Q3 turn on to conduct current. The conduction for both directions of inductor current $I_L > 0$ and $I_L < 0$ is shown in Figure 2-11 and Figure 2-12 respectively.[27]

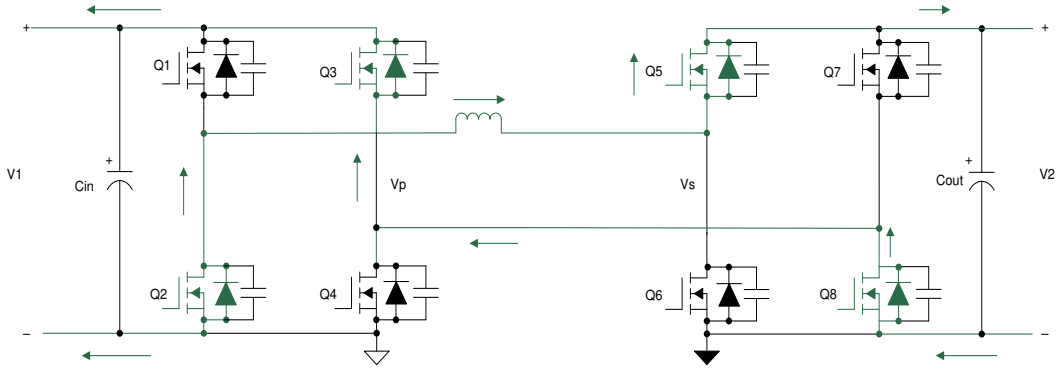


Figure 2.7: Interval 3: Positive Inductor Current

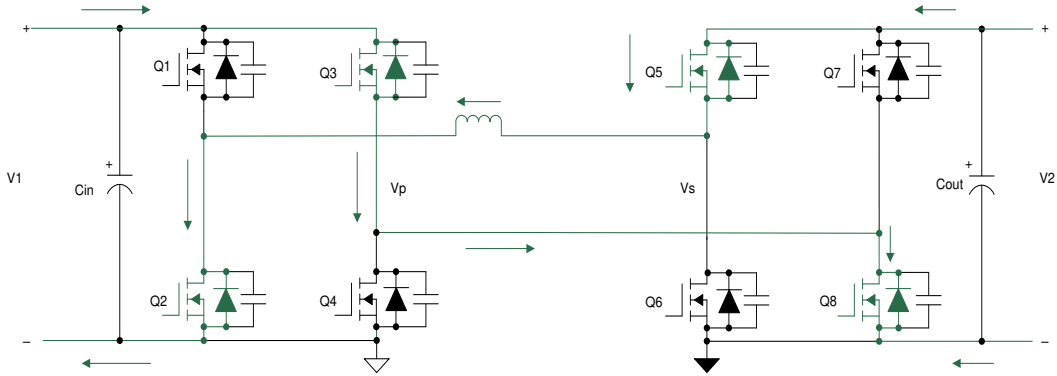


Figure 2.8: Interval 3: Negative Inductor Current

During interval four, the inductor current continues to be negative. During this interval, the voltage across the primary is $-V_1$ and, and the voltage across the secondary is $-V_2$. The difference in these voltages, which is $(-V_1 + V_2)$, appears across the inductor. Hence, the current ramps down with a negative slope as shown in Equation 5.[27]

$$\frac{di(t)}{dt} = -\frac{V_1 - V_2}{L} \quad (2.9)$$

During this interval, switches Q2 and Q3 continue to remain turned on, but as the voltage across the secondary are now $-V_2$, switches Q6 and Q7 turn on to conduct current as shown in Figure 2-13.[27]

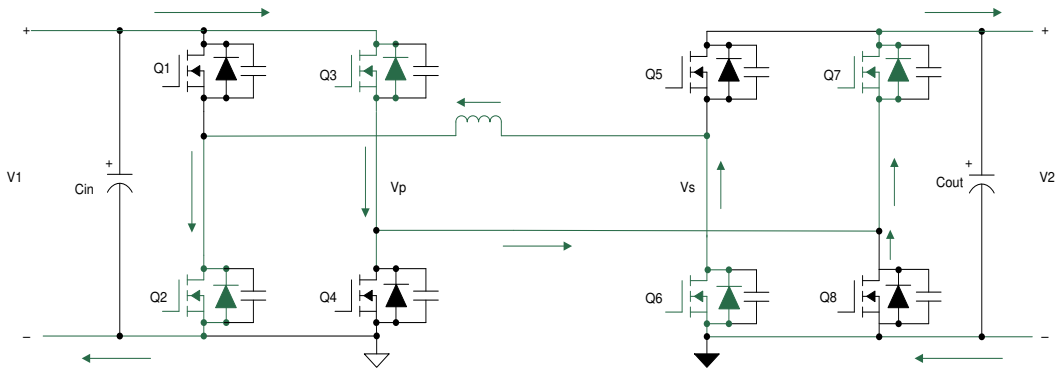


Figure 2.9: Interval 4

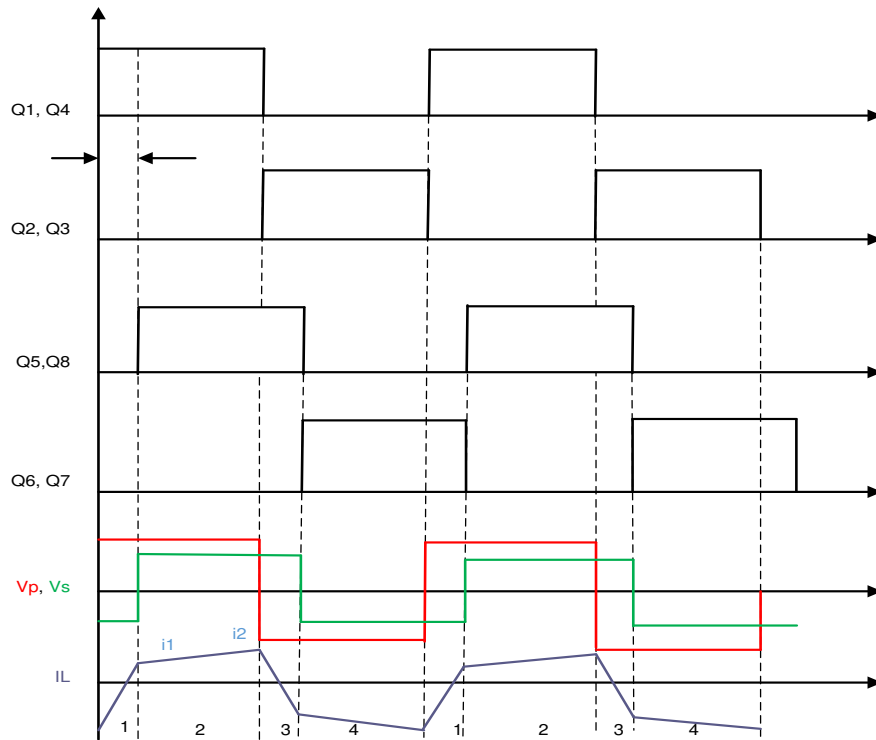


Figure 2.10: Gate Signals, Transformer Primary and Secondary Voltages, and Inductor Current

Figure 2-14 shows the gating pulses of the switches on the primary and secondary side. The variable ϕ represents the phase shift between the PWM pulses of the primary and secondary side. V_p and V_s represent the voltage on the primary and secondary winding of the transformer. I_L represents the transformer current.[27]

2.3.3 Dual-Active Bridge - Zero Voltage Switching (ZVS)

During the transition from interval one to two, there exists a small dead time where the inductor-stored energy discharges the output capacitances of the MOSFETs and holds them close to zero voltage before they are turned on. This phenomenon, where the voltage across the MOSFET is close to zero at turn on, is referred to as zero voltage switching (ZVS). This is a major advantage with this topology, where due to the natural lagging current in one of the bridges, the inductive stored energy causes ZVS of all of the lagging bridge switches and some of the switches of the leading bridge. This depends on the stored inductive energy ($E_L = \frac{1}{2}LI^2$) available to charge and discharge the output capacitances of MOSFETs ($EC = \frac{1}{2}CV^2$).

When transition happens from interval one to two, the primary side switches Q1 and Q5 continue conduction, whereas in the secondary, Q6 and Q7 turn off and Q5 and Q8 turn on. Initially the voltage across Q6 and Q7 is zero when they are conducting, and Q5 and Q8 block the entire secondary voltage. During dead time, when all of the switches in the secondary are off, the inductor-stored energy circulates current which discharges the capacitor across MOSFETs Q5 and Q8 to zero and charges the capacitor across MOSFETs Q6 and Q7 to the full secondary voltage. The current commutation is shown in Figure 2-15.[27]

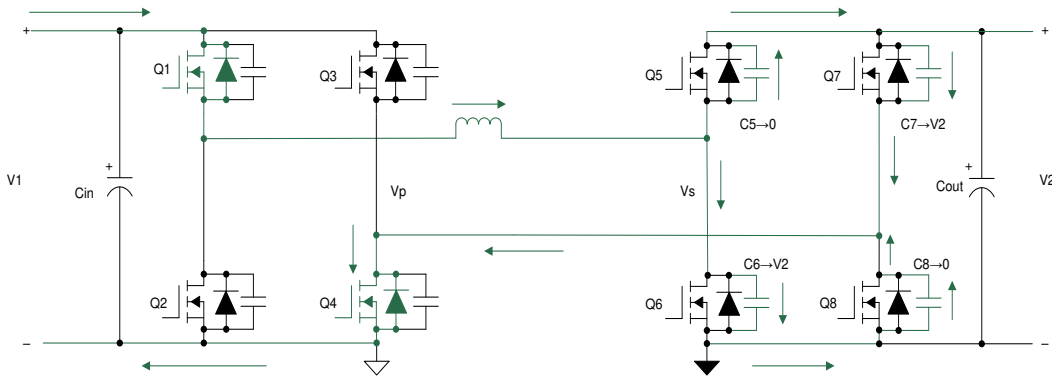


Figure 2.11: ZVS Transition in Secondary Side - Capacitor

Once the capacitors have been charged and discharged, the current must continue to flow. The current will flow through the diodes D5 and D8, thereby clamping the voltage across MOSFETs Q5 and Q8 to zero as shown in Figure 2-16. During the next

interval, MOSFETs Q5 and Q8 are turned on at zero voltage, thereby reducing turn on losses completely. The arrow close to the diode indicates that the diode is conducting and the MOSFET is off.[27]

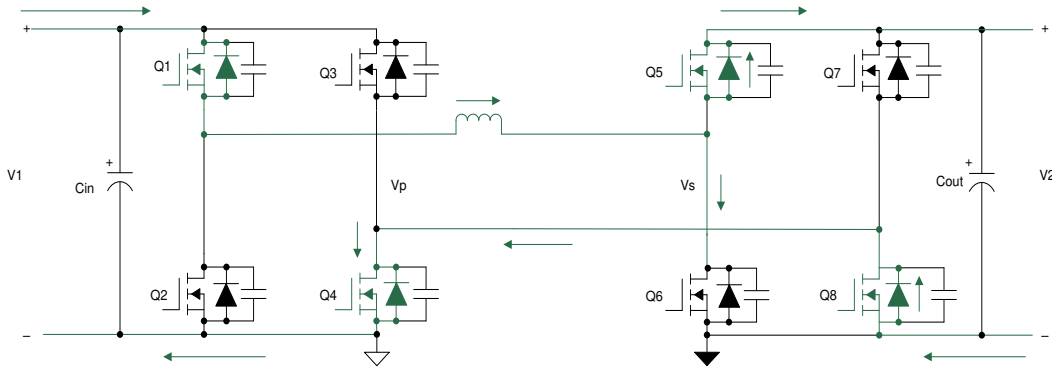


Figure 2.12: ZVS Transition in Secondary Side - Diode ZVS Transition in Secondary Side - Diode

Similarly, zero voltage switching across the switches of the primary during the transition from interval 2 to 3 is explained in the following section. When transition happens from interval two to three, the secondary side switches Q5 and Q8 continue conduction, whereas in the primary, Q1 and Q4 turn off and Q2 and Q3 turn on. Initially, the voltage across Q1 and Q4 is zero when they are conducting, and Q2 and Q3 block the entire secondary voltage. During dead time when all of the switches in the primary are off, the inductor stored energy circulates current, which discharges the capacitor across MOSFETs Q2 and Q3 to zero and charges the capacitor across MOSFETs Q1 and Q4 to the full primary voltage. The current commutation is shown in Figure 2-13.[27]

with

$$i_L(0) = \frac{1}{2L\omega} (V_s(\pi - 2\phi) - (V_e\pi)) \quad (2.11)$$

Mode2 [ϕ to π]:

$$i_L(t) = i_L(\phi) + \frac{V_e - V_s}{L} (\omega t - \phi) \quad (2.12)$$

with

$$i_L(\phi) = \frac{1}{2L\omega} (V_e\pi - V_s(\pi - 2\phi)) \quad (2.13)$$

- modeling the power throughput

$$P = \frac{1}{\pi} \left(\int_0^\pi V_e * I_L(t) dt \right) \quad (2.14)$$

$$P = \frac{V_e V_s}{n f L} \phi \left(1 - \frac{\phi}{\pi} \right) \quad (2.15)$$

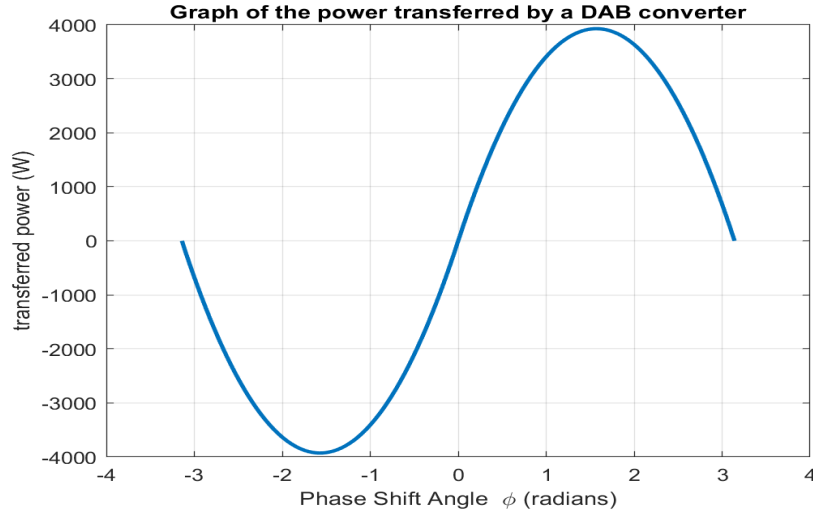


Figure 2.15: Power transfer in DAB converter in function of the phase shift

- Varying the duty ratio or the phase-shift between bridges adjusts the power flow
- The transmitted power is maximal when the angle reaches 90° or $\pi/2$

2.3.5 Output power calculation (In one direction)

In Figure 2.16, the output load is made of a resistor in parallel with a capacitor. In order to find the power " P_{out} " transferred from the input source to the output load, we need to find and draw : $V_L \rightarrow I_L \rightarrow I_0$ then we get the expression of P_{out} . After that we can obtain the expression of the conversion ratio m .

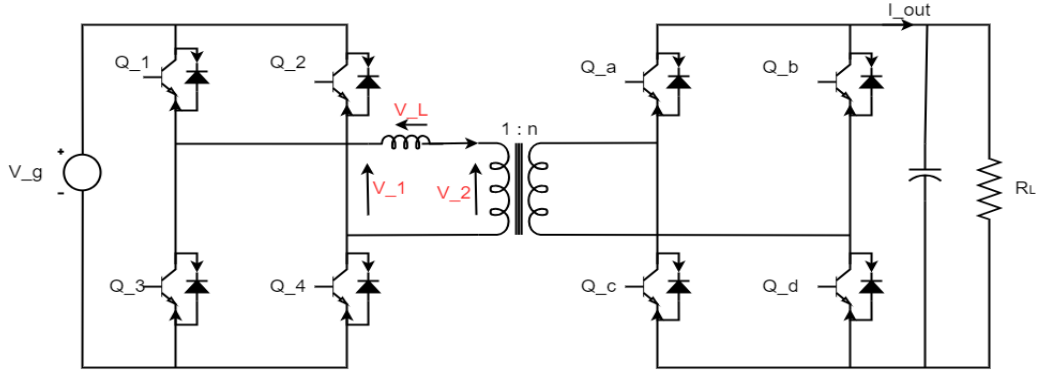


Figure 2.16: Dual Active Bridge (R_L load)

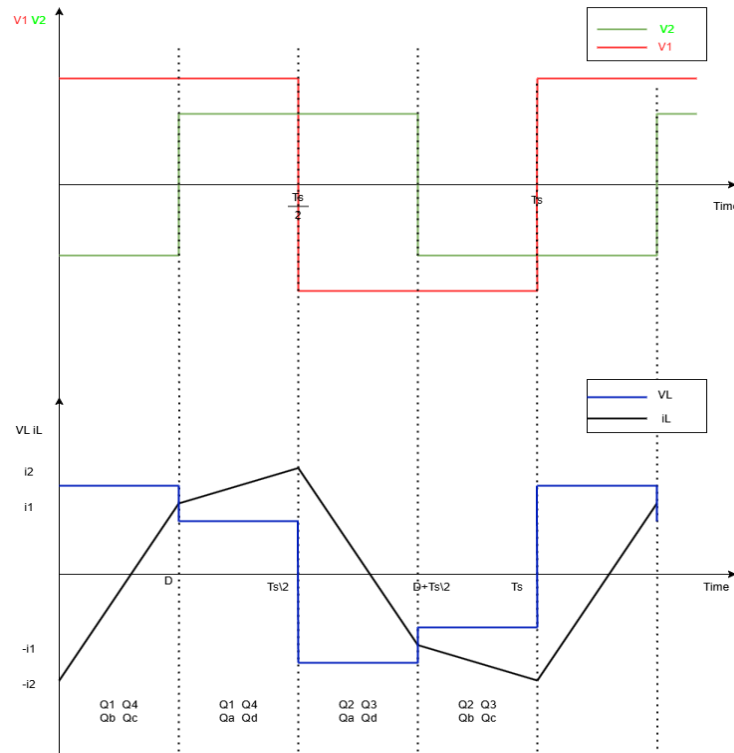


Figure 2.17: Wave curves of input voltage (V_1), output voltage (V_2), inductor voltage(V_L) and Current (i_L)

The average current of the inductor is null $\langle i_L \rangle = I_L = 0$ as there is no DC component.

To simplify calculation, we assume that $n=1$, and i_{out} is a rectified version of i_L

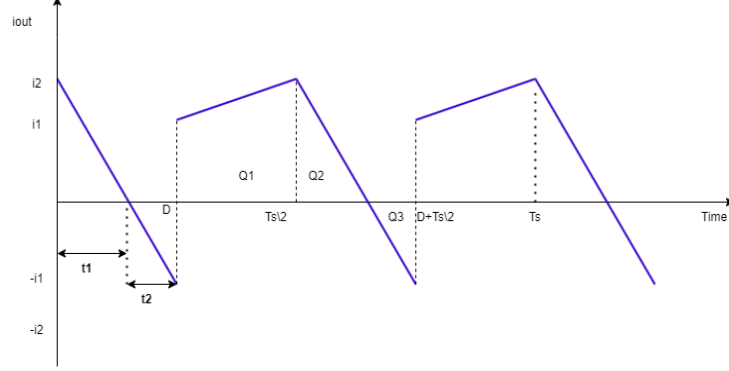


Figure 2.18: Output Current waveform

$$I_{out} = \frac{Q}{T_{s/2}} \quad (2.16)$$

We have:

$$I_2 = t_1 \frac{V_g + \frac{V_0}{n}}{L} \quad (2.17)$$

$$I_1 = t_2 \frac{V_g + \frac{V_0}{n}}{L} \quad (2.18)$$

$$\phi = t_1 + t_2 \quad (2.19)$$

$$I_1 + I_2 = (t_1 + t_2) \frac{V_g + \frac{V_0}{n}}{L} = \phi \frac{V_g + \frac{V_0}{n}}{L} \quad (2.20)$$

$$I_2 + I_1 = \left(\frac{T_s}{2} - \phi \right) \frac{V_g - \frac{V_0}{n}}{L} \quad (2.21)$$

Then:

$$Q = Q_1 + Q_2 + Q_3 \quad (2.22)$$

$$Q = \frac{1}{2} (I_1 + I_2) \left(\frac{T_s}{2} - \phi \right) + \frac{1}{2} t_1 I_2 - \frac{1}{2} t_2 I_1 \quad (2.23)$$

$$Q = \frac{1}{2} \left(\phi \frac{V_g + \frac{V_0}{n}}{L} \right) \left(\frac{T_s}{2} - \phi \right) + \frac{1}{2} \frac{1}{\frac{V_g + V_0/n}{L}} (I_2^2 - I_1^2) \quad (2.24)$$

$$Q = \frac{11}{22} \left(\phi \frac{V_g + \frac{V_0}{n}}{L} \right) \left(\frac{T_s}{2} - \phi \right) + \frac{1}{2} \phi \left(\frac{V_g - \frac{V_0}{n}}{L} \right) \left(\frac{T_s}{2} - \phi \right) \quad (2.25)$$

$$\Rightarrow Q = \frac{1}{2} \phi \left(\frac{T_s}{2} - \phi \right) \frac{2V_g}{L} \quad (2.26)$$

$$\Rightarrow Q = \left[\frac{V_g}{L} \phi \left(\frac{T_s}{2} - \phi \right) \right] \quad (2.27)$$

$$\langle i_{out} \rangle = I_{out} = \frac{Q}{T_s/2} = \frac{V_g \phi}{L \cdot T_s/2} \cdot \left(\frac{T_s}{2} - \phi \right) \quad (2.28)$$

$$I_{out} = \frac{V_g \phi}{L} \cdot \left(1 - \frac{\phi}{T_s/2} \right) \quad (2.29)$$

We define

$$D = \frac{\phi}{T_s/2} = 2\phi f_s \quad (2.30)$$

$$I_{out} = \frac{V_g D (1 - D)}{2L f_s} \quad (2.31)$$

When n is different than 1 $n \neq 1$, equation 2.31 becomes:

$$I_{out} = \frac{V_g D (1 - D)}{n \cdot 2L f_s} = \frac{V_o}{R_L} \quad (2.32)$$

$$P_{out} = V_{out} I_{out} \Rightarrow \frac{V_o V_g D (1 - D)}{2nL f_s} \quad (2.33)$$

The power flow depends on D , where $0 \leq D \leq 1$

The output power equation can also be written as follows:

$$P = \frac{V_g V_o}{n f_s L} \phi \left(1 - \frac{\phi}{\pi} \right) \quad (2.34)$$

The conversion ratio is then obtained by rearranging equation 2.33, It is given as:

$$m = \frac{V_0}{V_g} = \frac{R_L D(1 - D)}{2nL f_s} \quad (2.35)$$

2.3.6 DAB component selection

How to we choose n ? range of D ? L_L and C_0 ?

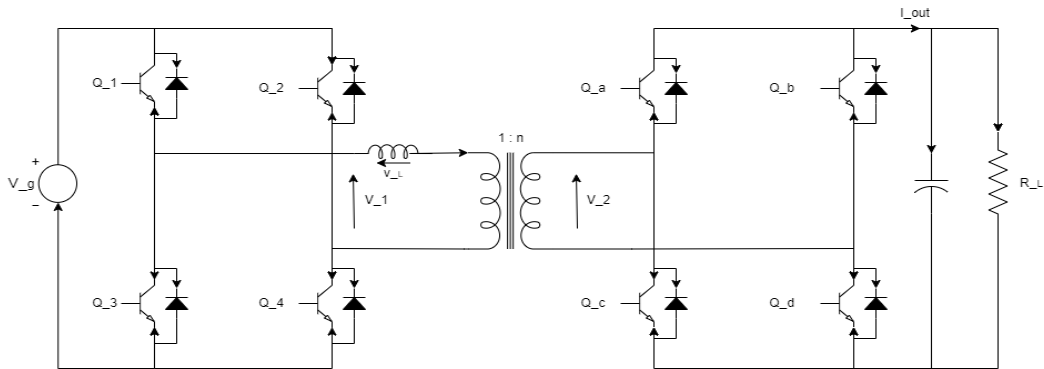


Figure 2.19: Dual Active Bridge R_L load

1- First, we start by choosing n

In this example we have:

- fixed input voltage
- fixed output voltage

We'll look at how i_L varies with n

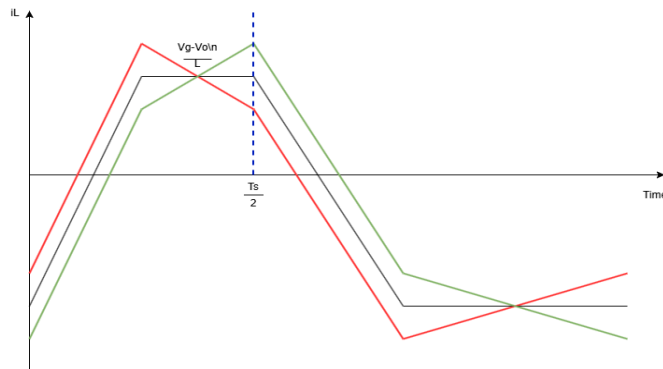


Figure 2.20: Three cases of i_L (inductance current)

$$\Rightarrow \text{case 1: } V_g > \frac{V_o}{n},$$

$$\Rightarrow \text{case 2: } V_g < \frac{V_o}{n}.$$

\Rightarrow case 3: $V_g = \frac{V_o}{n} \rightarrow$ this slope reduces the RMS current (reduces the peak current) \Rightarrow reduces conduction losses.

$$\Rightarrow \text{Ideal } n \text{ to choose is } n = \frac{V_o}{V_g}$$

Still we need to know:

- The range of D
- L_L
- C_0

First we need to know the limits of the output current : $I_{min} < i_0 < I_{max}$

if $D=D1$

$$I_0 = \frac{V_g D(1-D)}{2L_t f_s n} \longrightarrow I_{min} = \frac{V_g D_1(1-D_1)}{2L_f f_5 n}$$

if $D=D2$

$$I_0 = \frac{V_g D(1-D)}{2L_t f_s n} \longrightarrow I_{max} = \frac{V_g D_2(1-D_2)}{2L_2 f_5 n}$$

The maximum power we can transfer occurs at $D = 0.5$.

AT maximum load we should choose D_2 close to $D = 0.5$. We will not choose $D = 0.5$ exactly, we need a little room, and this for the following reasons:

- 1- We may need a little room for transits
2. the control action flips after $D = 0.5$, a case that musy be avoided.

Let's choose $D_2 = 0.4$, and find D_1 .

$$\frac{I_{min}}{I_{max}} = \frac{D1(1-D1)}{D2(1-D2)} \tag{2.36}$$

$$-D_1^2 + D_1 - C = 0;$$

$$C = D_2(1-D_2) \left(\frac{I_{min}}{I_{max}} \right);$$

$$\Delta = b^2 - 4ac = 1 - 4c$$

$$D_1 = \frac{-b - \sqrt{\Delta}}{2} = \frac{-1 - \sqrt{1 - 4c}}{-2}$$

$$D_1 = \frac{-b + \sqrt{\Delta}}{2} = \frac{-1 + \sqrt{1 - 4c}}{-2}$$

We choose $0 < D_1 < D_2 \Leftrightarrow 0 < D_1 < 0,4$

$L_L = ?$

$$I_{\max} = \frac{V_g D_2 (1 - D_2)}{2L_L f_s n}$$

$$L_L = \frac{V_g D_2 (1 - D_2)}{2I_{\max} f_s n} \quad (2.37)$$

Now, How to find C_o ?

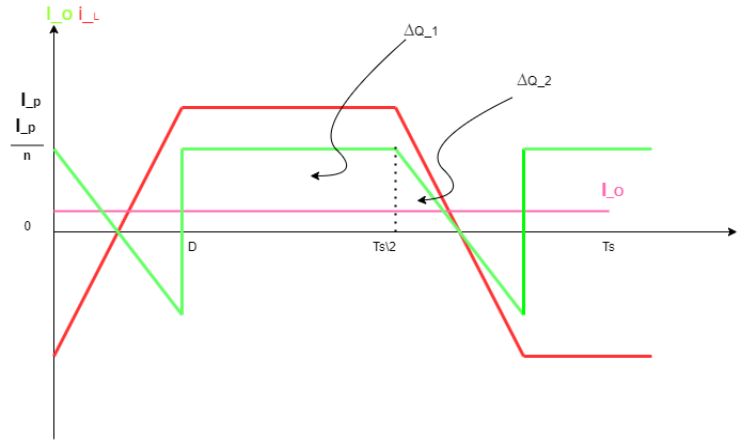


Figure 2.21: Wave curves of inductor current (i_L), Output current(i_o) and output average current (I_o)

$I_0 = \langle i_0(t) \rangle$ is the average current of $i_0(t)$

$$C_0 = \frac{\Delta Q}{2\Delta V_0} \quad (2.38)$$

$$\Delta Q = \Delta Q_1 + \Delta Q_2 \quad (2.39)$$

$$\Delta Q_1 = \left(\frac{I_p}{n} - I_0 \right) \left(\frac{T_s}{2} - \phi \right) \quad (2.40)$$

$$\Delta Q_2 = \frac{1}{2} \left(\frac{I_p}{n} - I_0 \right)^2 \left(\frac{I_p}{n} - I_0 \right) \frac{\phi/2}{I_p/n} = \frac{1}{2} \left(\frac{I_p}{n} - I_0 \right) \frac{\phi}{2} \cdot \frac{n}{I_p} \quad (2.41)$$

We Know that: $I_0 = \frac{V_g D(1-D)T_s}{2L_L n}$;

$$\phi = \frac{DT_s}{2}$$

$$\text{So } \frac{I_p}{n} = \frac{V_g + \frac{V_0}{n}}{L_L} \cdot \frac{\phi}{2n} = \frac{V_g + \frac{V_0}{n}}{L_L} \cdot \frac{DT_s}{4n}$$

as we selected $n = \frac{V_0}{V_g} \Rightarrow V_g = \frac{V_0}{n}$ then $\frac{I_p}{n}$ becomes: $I_p = \frac{V_s DT_s}{2L_L h}$

$$\Delta Q_1 = \frac{V_g T_s^2 D^2 (1-D)}{4L_L n} \quad (2.42)$$

$$\Delta Q_2 = \frac{V_g T_s^2 D^2}{4L_L n} \quad (2.43)$$

$$\Delta Q = \Delta Q_1 + \Delta Q_2 \quad (2.44)$$

$$\Delta Q = \frac{V_g D^2 T_s^2}{4L_L n} \left[(1-D) + \frac{D^2}{4} \right] \quad (2.45)$$

What D do we choose to size C_o ? We want to find the case where ΔQ is max.

$$\frac{d\Delta Q}{dD} = 0 = \frac{d}{dD} \left(D^2 - D^3 - \frac{1}{4}D^4 \right) = D^3 - 3D^2 + 2D = 0 \quad (2.46)$$

$$D(D^2 - 3D + 2) = 0 \quad (2.47)$$

$$\begin{cases} D = 0 \\ D = 1 \\ D = 2 \text{ doesn't work} \end{cases} \quad (2.48)$$

$$\Delta = b^2 - 4ac \quad (2.49)$$

$$D_1 = \frac{-b + \sqrt{\Delta}}{2a} \quad (2.50)$$

$$D_2 = \frac{-b - \sqrt{\Delta}}{2a} \quad (2.51)$$

We look at the second derivative:

$$\frac{d^2 \Delta Q}{dD^2} = 2 - 6D + 3D^2 \Big|_{D=1} = -1 \quad (\text{negative}) \quad (2.52)$$

$$\frac{d^2 \Delta Q}{dD^2} = 2 - CD + 3D^2 \Big|_{D=0} = 2 \quad (\text{positive}) \quad (2.53)$$

This means that the worst case (or the largest ΔQ) is going to happen when D is maximum. (at maximum power) For this particular case we size C_o (at $D_{\max} = 0,4$)

$$C_o = \frac{\Delta Q|_{D=0,4}}{2\Delta v_0} \quad (2.54)$$

2.4 Open Loop simulation

2.4.1 System and simulation configuration

A MATLAB/SIMULINK is used to implement the Bidirectional DAB converter. Table 2.1 displays the parameter used in the simulation.

F (Hz)	10000* π
L (μ H)	0.0102
C (μ F)	4500
V_b (V)	250
V_e (V)	1000

Table 2.1: Component/parameter values

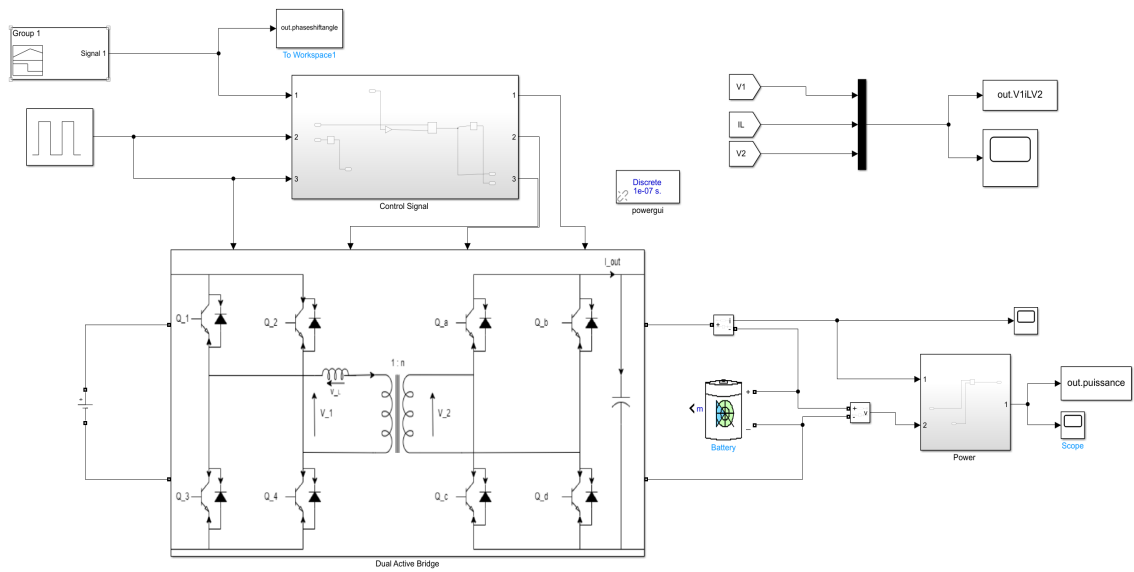


Figure 2.22: Simulation Open Loop of DAB converter

In this simulation, we used an IGBT transistor, RLC Branch, battery, linear transformer, DC voltage source, and a variable time delay.

2.4.2 Simulation results

In the first step, Different angles are chosen as a control signal to see the effect on the output voltage and current..

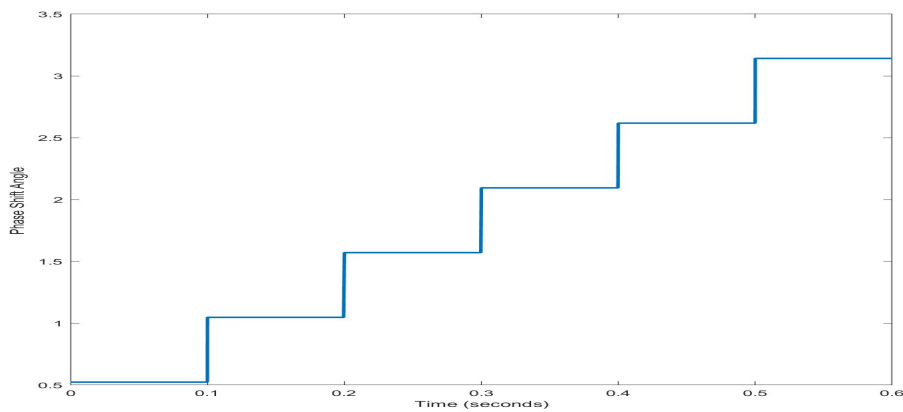


Figure 2.23: Phase shift angle

The variations in the current of the inductance, as well as the output voltage of the

The phase shift angle θ	$\pi/6$	$\pi/3$	$\pi/2$	$5\pi/6$	$2\pi/3$	π
--------------------------------	---------	---------	---------	----------	----------	-------

Table 2.2: Angle values

first bridge and the input voltage of the second bridge, are shown in Figure 2.24

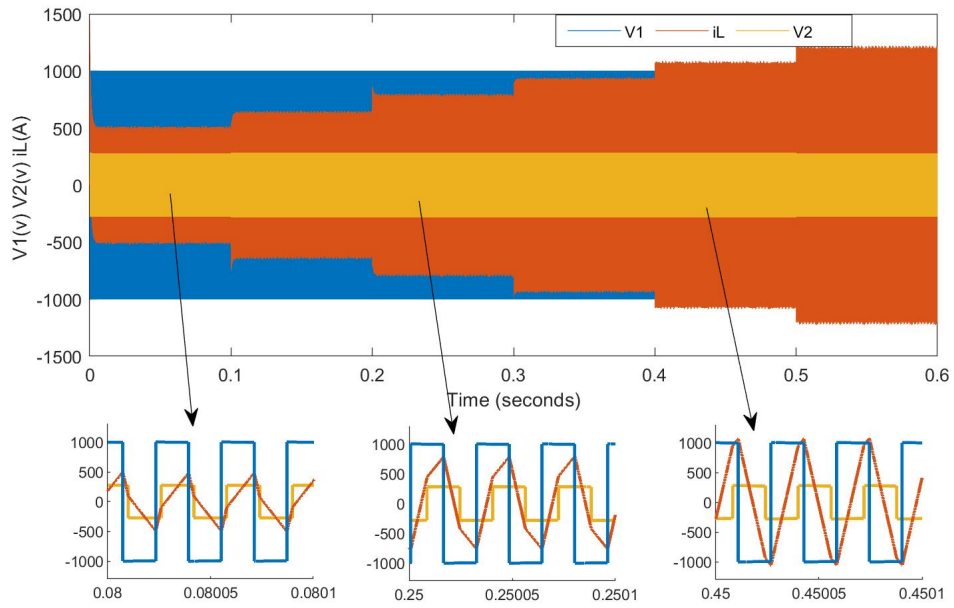


Figure 2.24: Current of the inductance (i_L), input voltage (V_1) and output voltage (V_2)

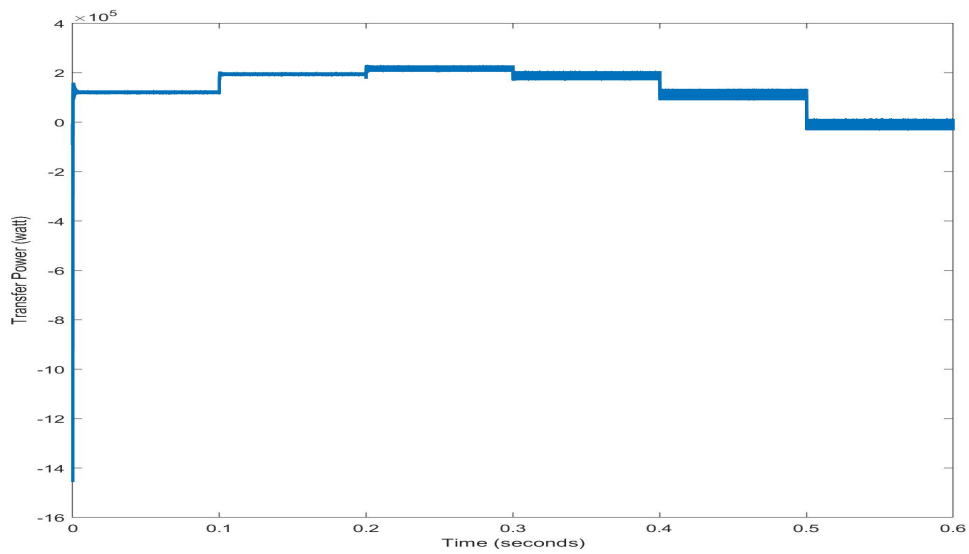


Figure 2.25: Output Power

The power changes are shown in Figure 2.25. we can see that the maximal transmitted power is when the angle reaches 90° or $\pi/2$ and it can be observed that the system has two phase shift angles that give the same power value, but the difference resides in the oscillations. The best one is when oscillations are minimum.

2.5 Summary

This chapter delves into the structure and operation of the Dual Active Bridge (DAB) converter, a critical component for EV charging stations. The DAB converter enables bidirectional power flow between the EV battery and the grid, making it highly suitable for V2G applications. The chapter describes the basic configuration of the DAB, including its primary and secondary bridges, and the isolation transformer that connects them. A detailed explanation of the DAB's switching sequence and Zero Voltage Switching (ZVS) mechanism is provided, emphasizing how ZVS reduces switching losses and improves overall system efficiency.

The power transfer process within the DAB is analyzed, with a focus on how phase shifts between the primary and secondary bridges control the direction and magnitude of power flow. The chapter also covers key design considerations, such as selecting appropriate component ratings and ensuring optimal operating conditions. Simulation results are presented to validate the theoretical analysis, showcasing the DAB's performance under various load conditions.

Chapter 3

DAB Charger Control

3.1 Introduction

A Dual Active Bridge (DAB) converter is a type of DC-DC converter that efficiently transfers power between two voltage levels. It is widely used in applications like battery storage and renewable energy systems. To control the power transfer in a DAB converter, a PID controller is often used. The PID controller adjusts the phase shift between the converter's primary and secondary bridges to match the desired power output.

3.2 Problem statement

This chapter focuses on the control of the DAB converter which is a part of an OnBoard EV charger. The topology of the studied single phase charger is presented in Figure 3.1

The main advantages of this topology compared to traditional topologies are:

- Two-stage structure of High Frequency (HF) conversion (compared to three stages for conventional topologies)
- Little capacitive storage on the DC bus and less passive components (less cost)

Despite the simple design and implementation, the main drawback of the DAB topology is the limited voltage operation range with the phase shift control. As output or

input voltages move away from the nominal operation, a large circulating energy arises between the bridges, conduction losses rise, and the soft-switching range is reduced, leading to a significant reduction in efficiency . Therefore, the resonant topologies, such as the LLC topology , are proposed to provide reduced peak currents, higher efficiency, and improved soft-switching range. Actually, the DAB converter uses the energy that is stored in its inductor L (which, in some designs, may be the transformer’s leakage inductance) to accomplish ZVS. Since the load current is the only factor affecting this energy, ZVS can be lost under a specific load depending on the value of L . In contrast, the DC-DC LLC converter achieves ZVS by using the energy stored in the magnetizing inductance of its transformer. Therefore, once the magnetizing inductance is established to achieve ZVS at a certain output voltage, it is maintained for all loads. Thus, in the comparison of DC-DC topologies, between control, design, efficiency requirements, and the cost should be taken into account in order to define the charger topology. the isolated DAB converter responsible to ensure the stability of the DC bus via the proposed control strategy.[16]

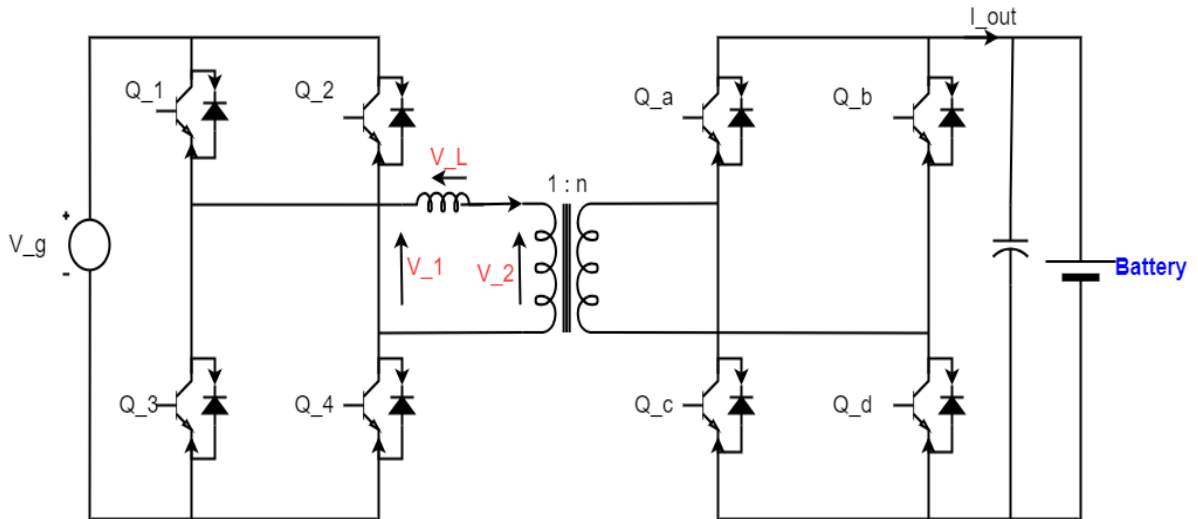


Figure 3.1: Dual Active Bridge

According to Figure 3.1, the single-phase DAB converter is made up of two H-bridges coupled by a HF AC transformer with a turns ratio of n . V_{DC} is the DC bus voltage, while V_b is the battery voltage. The AC voltages at the primary and secondary sides of the transformer are V_1 and V_2 respectively. L is the DAB inductor which serves

as the energy transfer element. The difference between the AC voltages of the input and output bridges, or V_1 and V_2 respectively, drives the current which flows in the inductor L . The HF transformer can achieve the galvanic isolation which increases the protection and guarantees that charging regulations are met in high voltage applications like EV chargers. The full bridge on the left side is connected to the High Voltage (HV) DC bus (Output of the previous stage (rectifier)) and the full bridge on the right side is connected to the battery.

3.3 Closed loop control

3.3.1 Design of PI control

PI control of a Dual Active Bridge (DAB) converter with power request involves regulating the phase shift between the primary and secondary bridges to achieve the desired power transfer. The PI controller adjusts the phase shift to minimize the error between the actual and requested power. By tuning the proportional, integral gains, the controller ensures stable and efficient power transfer.

Here is the equation of PI controller :

$$PI = K_p e(t) + K_i \int e(t) dt$$

To achieve the gains of our pi, we adjusted it using the method of trial and error.

Method of trial and error

The method of trial and error (or trial and testing) is a heuristic approach often used to tune Proportional-Integral (PI) controller gains. This method relies on manual adjustments of the controller parameters, observing the system's behavior, and iterating until acceptable performance is achieved.

The process to tune PI controller gains through trial and error generally involves the following steps:

1. **Start with zero gains:** Set both K_p and K_i to zero to ensure the system is stable before tuning.

2. **Adjust the proportional gain (K_p):** Gradually increase K_p until the system responds quickly, but without excessive oscillations.
3. **Adjust the integral gain (K_i):** After K_p is set, increase K_i to eliminate any steady-state error, while avoiding oscillations.
4. **Observe and fine-tune:** Continue adjusting both K_p and K_i as needed to reduce oscillations and achieve a stable response.
5. **Test the system:** Test the controller under different conditions and make adjustments if necessary.
6. **Refine the settings:** Keep tweaking K_p and K_i to meet performance criteria like response time, stability, and minimal overshoot.

Block diagram Closed loop system

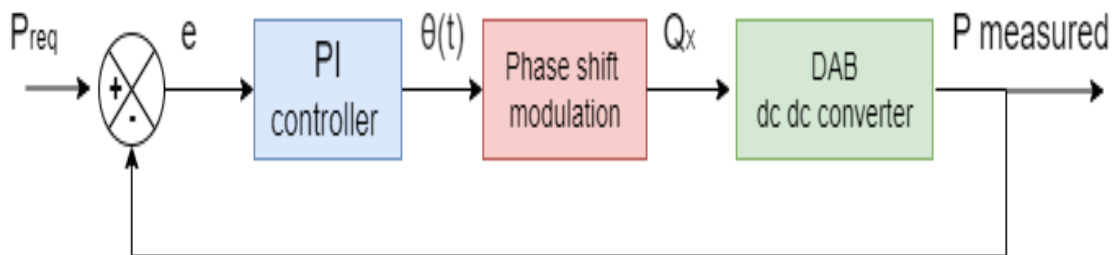


Figure 3.2: Block diagram of our closed loop system

3.3.2 System and simulation configuration

We use MATLAB/SIMULINK to implement our circuit Bidirectional DAB converter. Table 3.1 displays the parameter settings

To calculate DAB component C and L we use equation 2.46 and 2.36 respectively we obtain

- $C_{min}=47860 \mu\text{F}$
- $L=26.539 \mu\text{H}$

F (Hz)	$10000 * \pi$
L (μ H)	26.539
C (μ F)	48000
V_b (V)	250
V_e (V)	1000
K_p	0.000085
K_i	0.25

Table 3.1: Component/Parameter values

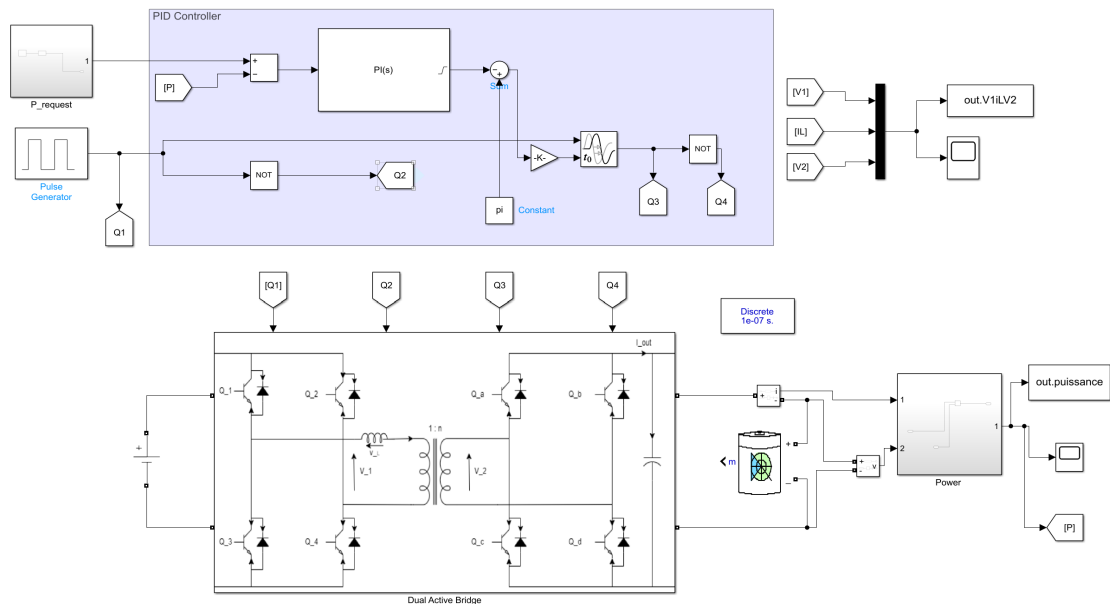


Figure 3.3: Simulation Closed Loop of DAB converter

In this simulation, we used an IGBT transistor, RLC Brqnc, battery, linear transformer, DC voltage source, variable time delay and a PI controller.

3.3.3 Simulation results

For this simulation, the power request] is presented in Figure 3.4 where it increases to reach 75000 W.

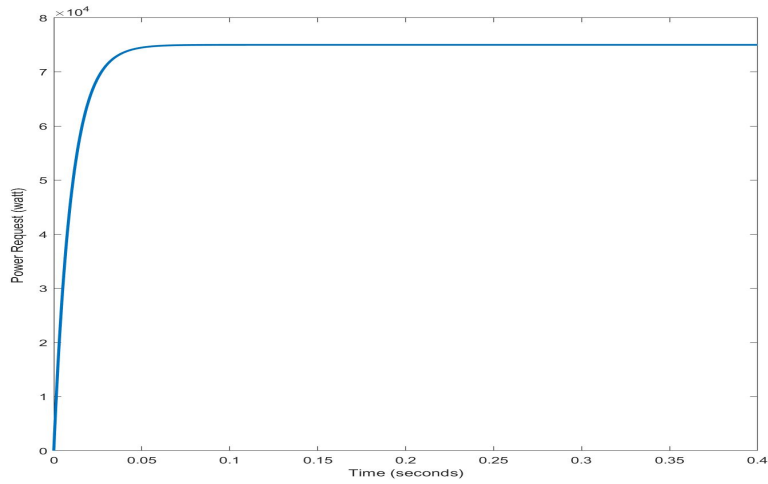


Figure 3.4: Power request

The controlled phase shift angle, presented in figure (3.5), and a zoom of the main waveforms of the IGBTs' signals of the DAB converter (Q1 and Q5) are presented in Figures 3.6.

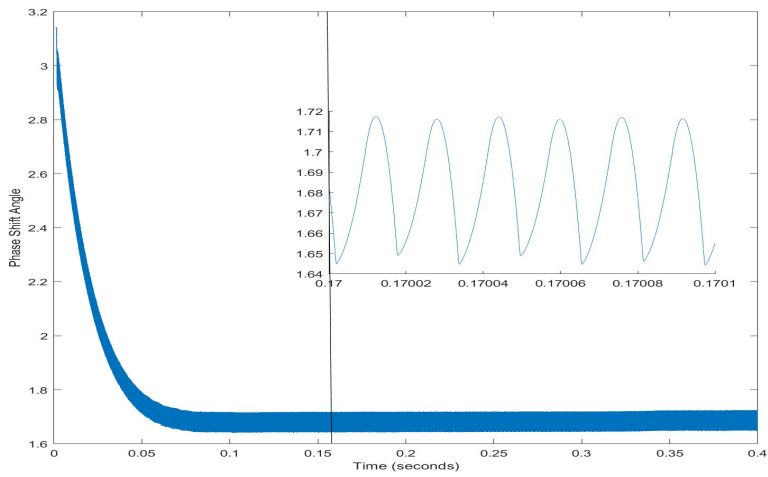


Figure 3.5: Phase shift angle

The controlled phase shift angle is crucial for optimizing the power transfer in the converter. By adjusting this angle, we can effectively manage the timing of the IGBT switches, impacting the overall efficiency of the system

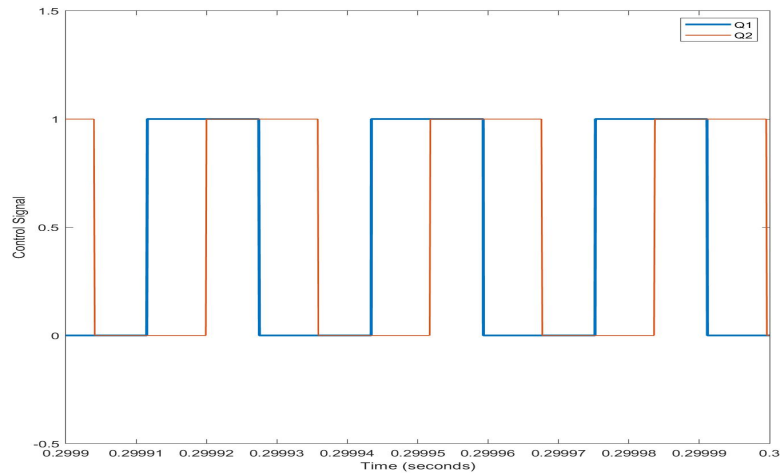


Figure 3.6: IGBTs' waveforms with SPS in G2V mode for $V_b=250V$ and $P=7,5kW$

The waveforms of the IGBTs (Q1 and Q5) under specific conditions (G2V mode, $P=7.5kW$, $v_b=250V$) reveal the switching behavior of the devices. Analyzing these waveforms helps in understanding the dynamic response of the converter and identifying any potential issues related to switching losses or delays

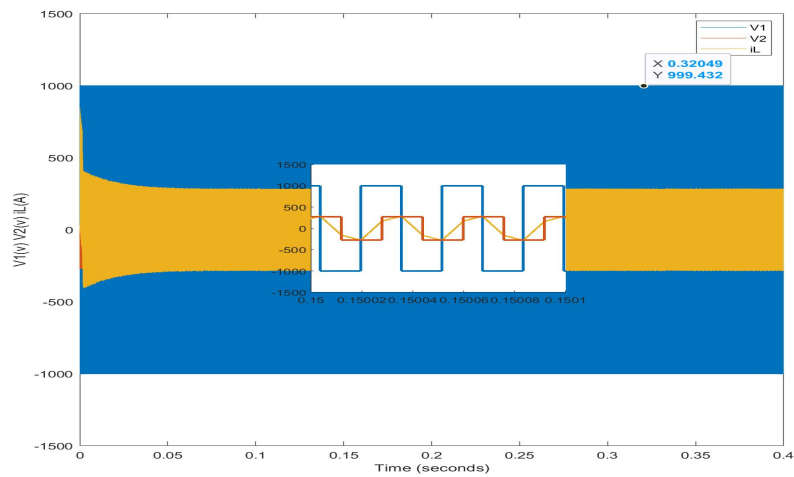


Figure 3.7: current of the inductance(i_L), output voltage of the first bridge(V_1), the input voltage of the second bridge(V_2)

This figure illustrates the relationship between the inductance current(i_L) and the voltages across the bridges(V_1 and V_2) Monitoring these parameters is essential for

ensuring stable operation and effective energy transfer between the two sides of the converter.

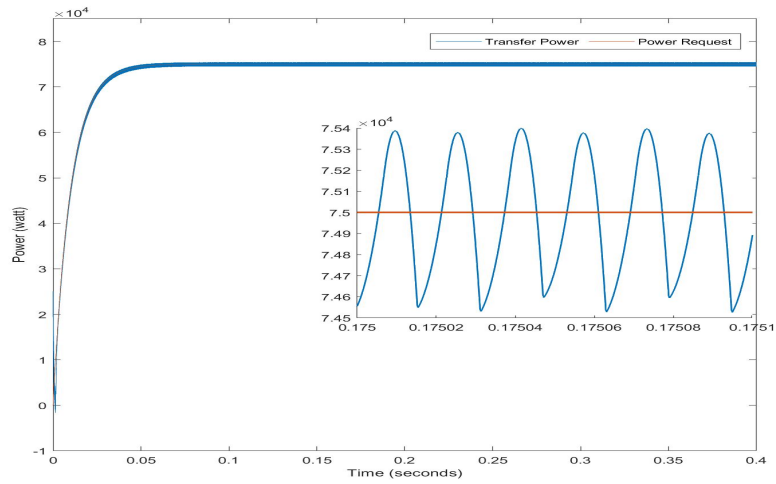


Figure 3.8: Comparison between power request and transfer power

in figure 3.8 The comparison between power request and actual transfer power provides valuable insights into the converter's responsiveness. The close alignment between these two metrics indicates that the converter is effectively tracking the power demand, which is critical for applications requiring precise power management.

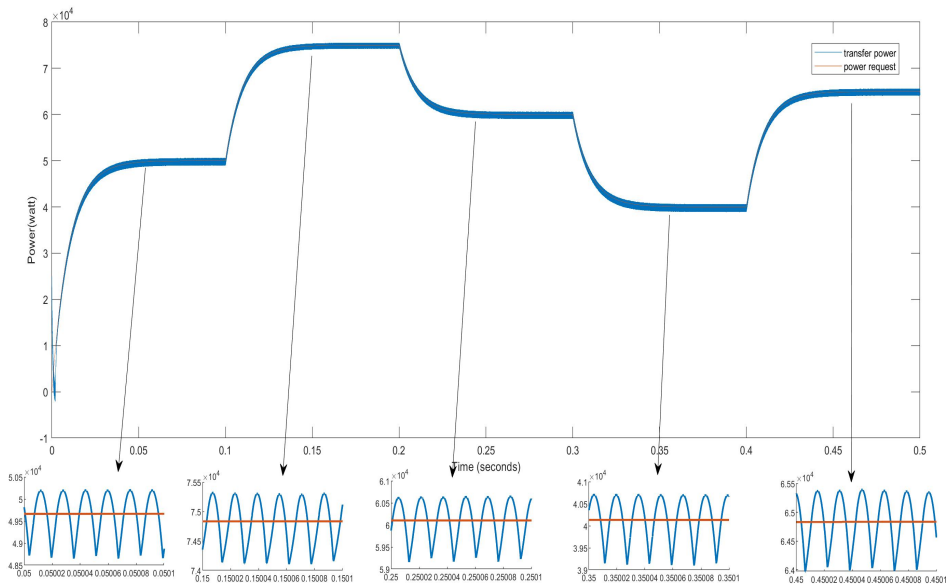


Figure 3.9: Comparison between power request and actual transferred power

in figure 3.9 The comparison between different power request and actual transferred power provides valuable insights about the converter's response and accuracy. The close alignment between these powers indicates that the converter is effectively tracking the power demand, which is critical for applications requiring precise power management.

3.4 Summary

In this chapter, the focus shifts to the control strategies implemented in the DAB converter to ensure stable and efficient operation in EV charging stations. The chapter begins by outlining the challenges associated with controlling the DAB, particularly in managing the dynamic power demands of EVs during charging and discharging. The proposed control scheme is based on phase-shift modulation, which adjusts the phase angle between the primary and secondary bridges to regulate power flow.

The control system is further enhanced with a Proportional-Integral (PI) controller, which stabilizes the output by minimizing the error between the requested power and the actual power delivered. Detailed simulations are conducted to assess the effectiveness of the control strategy, demonstrating improvements in system stability and response time. The results show that the PI-controlled DAB converter can efficiently manage bidirectional power flow, making it a reliable solution for future EV charging stations.

General Conclusion

This thesis has explored the analysis and control of the Dual Active Bridge (DAB) converter as a critical component for electric vehicle (EV) charging stations. The research demonstrated that the DAB converter's bidirectional power flow capability, combined with galvanic isolation, makes it an ideal choice for applications requiring efficient energy transfer between the grid and EV batteries. The study emphasized the importance of phase-shift control strategies and the implementation of Zero Voltage Switching (ZVS) to optimize performance and minimize energy losses.

Simulation results validated the theoretical analysis, showing that the DAB converter can handle high power levels while maintaining stable operation in both charging and discharging modes. The introduction of the PI controller further improved the system's performance, reducing response time and enhancing stability during dynamic power exchanges.

Overall, the work presented in this thesis contributes to the development of advanced EV charging infrastructure. The findings demonstrate that the DAB converter, with proper control strategies, can significantly enhance the efficiency and reliability of EV charging stations, supporting the growing adoption of electric vehicles and the integration of renewable energy sources into the power grid. Future research could explore further optimization of the control system and investigate the scalability of the DAB converter for different power levels and EV charging scenarios.

Bibliography

- [1] Iqbal Husain. Electric and hybrid vehicles: design fundamentals. CRC press, 2021.
- [2] Chunhua Liu; K. T. Chau; Diyun Wu; Shuang Gao. Opportunities and challenges. Proceedings of the IEEE, 2013.
- [3] Auke Hoekstra and Pavol Bauer. Electric Cars: Technology. edX, 2023.
- [4] Mohammad Kebriaei, Abolfazl Halvaei Niasar, and Behzad Asaei. Hybrid electric vehicles: An overview. In 2015 International Conference on Connected Vehicles and Expo (ICCVE), pages 299–305. IEEE, 2015.
- [5] Aviru Kumar Basu, Shreyansh Tatiya, and Shantanu Bhattacharya. Overview of electric vehicles (evs) and ev sensors. Sensors for automotive and aerospace applications, pages 107–122, 2019.
- [6] Maria Carmen Falvo, Danilo Sbordone, I. Safak Bayram, and Michael Devetsikiotis. Ev charging stations and modes: International standards. In 2014 International Symposium on Power Electronics, Electrical Drives, Automation and Motion, pages 1134–1139, 2014.
- [7] Rajanand Patnaik Narasipuram and Subbarao Mopidevi. A technological overview and design considerations for developing electric vehicle charging stations. Journal of Energy Storage, 43:103225, 2021.
- [8] I Sami, Z Ullah, K Salman, I Hussain, SM Ali, B Khan, CA Mehmood, and U Farid. A bidirectional interactive electric vehicles operation modes: Vehicle-to-grid (v2g) and grid-to-vehicle (g2v) variations within smart grid. In 2019

- international conference on engineering and emerging technologies (ICEET), pages 1–6. IEEE, 2019.
- [9] Deepak Ravi, Bandi Mallikarjuna Reddy, SL Shimi, and Paulson Samuel. Bidirectional dc to dc converters: an overview of various topologies, switching schemes and control techniques. International Journal of Engineering & Technology, 7(4.5):360–365, 2018.
- [10] H.R. Karshenas, H. Daneshpajoo, A. Safae, P. Jain, and A. Bakhshai. Bidirectional dc-dc converters for energy storage systems. In Energy Storage in the Emerging Era of Smart Grids, volume 18. IntechOpen, London, UK, 2011.
- [11] S. Wang, Z. Zheng, C. Li, L. Xu, K. Wang, and Y. Li. Accurate frequency-domain analysis and hybrid control method for isolated dual active bridge series resonant dc/dc converters. IET Power Electronics, 12:2932–2941, 2019.
- [12] H. Bai and C. Mi. Eliminate reactive power and increase system efficiency of isolated bidirectional dual-active-bridge dc–dc converters using novel dual-phase-shift control. IEEE Transactions on Power Electronics, 23(6):2905–2914, 2008.
- [13] W. Zhifu, W. Yupu, and R. Yinan. Design of closed-loop control system for a bidirectional full bridge dc/dc converter. Applied Energy, 194:617–625, 2017.
- [14] R. Pramanik and B. Pati. Modelling and control of a non-isolated half-bridge bidirectional dc-dc converter with an energy management topology applicable with ev/hev. Journal of King Saud University - Engineering Sciences, 2021.
- [15] S.A. Gorji, H.G. Sahebi, M. Ektesabi, and A.B. Rad. Topologies and control schemes of bidirectional dc–dc power converters: An overview. IEEE Access, 7:117997–118019, 2019.
- [16] Houssein Al Attar. Bidirectional Electric Vehicle Charger Control. PhD thesis, École centrale de Nantes, 2022.
- [17] Saman A. Gorji, Hosein G. Sahebi, Mehran Ektesabi, and Ahmad B. Rad. Topologies and control schemes of bidirectional dc–dc power converters: An overview. IEEE Access, 7:117997–118019, 2019.

- [18] B.M. Reddy and P. Samuel. A comparative analysis of non-isolated bi-directional dc-dc converters. In Proceedings of the IEEE 1st International Conference on Power Electronics, Intelligent Control and Energy Systems (ICPEICES), pages 1–6, Delhi, India, July 4–6 2016. IEEE.
- [19] M.C. Joshi and S. Samanta. Modeling and control of bidirectional dc-dc converter fed pm dc motor for electric vehicles. In Proceedings of the Annual IEEE India Conference (INDICON), pages 1–6, Mumbai, India, December 13–15 2013. IEEE.
- [20] N. Bodravara, S. Malapur, and M.B. Shruthi. Comparison of isolated and non-isolated bidirectional dc-dc converter fed pm dc motor. International Journal of Research in Applied Science and Engineering Technology (IJRASET), 3:698–702, 2015.
- [21] J. Lee, Y. Jeong, and B. Han. A two-stage isolated/bidirectional dc/dc converter with current ripple reduction technique. IEEE Transactions on Industrial Electronics, 59:644–646, 2012.
- [22] Y.-E. Wu and Y.-T. Ke. A novel bidirectional isolated dc-dc converter with high voltage gain and wide input voltage. IEEE Transactions on Power Electronics, 36:7973–7985, 2021.
- [23] T. Hirose and H. Matsuo. A consideration of bidirectional superposed dual active bridge dc-dc converter. In Proceedings of the 2nd International Symposium on Power Electronics for Distributed Generation Systems, pages 39–46, Hefei, China, June 16–18 2010.
- [24] X. Pan, H. Li, Y. Liu, T. Zhao, C. Ju, and A.K. Rathore. An overview and comprehensive comparative evaluation of current-fed isolated bidirectional dc/dc converter. IEEE Transactions on Power Electronics, 35:2737–2763, 2019.
- [25] Jacob A. Mueller and Jonathan W. Kimball. An improved generalized average model of dc–dc dual active bridge converters. IEEE Transactions on Power Electronics, 33(11):9975–9988, 2018.

- [26] Kalpana Meena, Kuldeep Jayaswal, and D. K. Palwalia. Analysis of dual active bridge converter for solid state transformer application using single-phase shift control technique. In 2020 International Conference on Inventive Computation Technologies (ICICT), pages 1–6, 2020.
- [27] L Song, H Ramakrishnan, N Navaneeth Kumar, and M Bhardwaj. Bi-directional, dual active bridge reference design for level 3 electric vehicle charging stations. Texas Instruments, Tech. Rep., 2019.